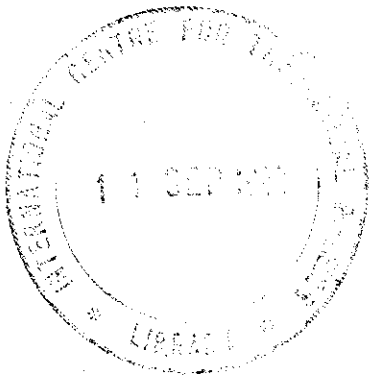

INTERNATIONAL ATOMIC ENERGY AGENCY
UNITED NATIONS EDUCATIONAL, SCIENTIFIC AND CULTURAL ORGANIZATION

INTERNATIONAL CENTRE FOR THEORETICAL PHYSICS
34100 TRIESTE (ITALY) - P.O.B. 586 - MIRAMARE - STRADA COSTIERA 11 - TELEPHONES: 224281/2/3/4/5/6
CABLE: CENTRATOM - TELEX 460392-1

SMR/113 - 9

AUTUMN COLLEGE

ON

THE TROPOSPHERE, STRATOSPHERE AND MESOSPHERE

10 September - 19 October 1984

RADIO WAVE PROPAGATION IN THE TROPOSPHERE.

SCATTERING AND DIFFRACTION.

D.T. GJESSING

Royal Norwegian Council for Scientific
and Industrial Research
Kjeller
Norway

INTERNATIONAL CENTER FOR THEORETICAL PHYSICS

Trieste Course (Sept - Oct, 1984)

on

RADIO WAVE PROPAGATION IN THE TROPOSPHERE. SCATTERING AND DIFFRACTION

by

Dag T Gjessing

Royal Norwegian Council for Scientific and Industrial Research
Environmental Surveillance Technology Programme
and
University of Tromsö
Institute of Mathematical and Physical Sciences

1 INTRODUCTION

The progress in radio science in general and wave propagation in particular during the last decade has been remarkable. At first this progress was stimulated primarily by interests in radio communications and military needs. Then there was a period when space research was a driving force. Now the progress is much a result of an upsurge of interest in problems concerned with environmental sciencies, by earth resources, pollution and conservation.

In parallel with this general progress in radio science, we are witnessing a development towards a new generation of powerful technology, a new generation of devices and concepts.

Solid state microwave sources can efficiently be controlled by microprocessors to give a specific field configuration. Dynamic matched receiver filtering is provided by devices based on surface acoustic waves. New opto-acoustic systems together with

charge-coupled devices hold great promise in regard to intricate on-line processing and pattern recognition.

The radio scientist is facing a challenging and inspiring future, one of matching new technological achievements to a wide field of applications making use of radio wave propagation.

These new technological achievements make it possible to optimize the usage of the propagation medium for the desired application. To achieve this optimization, however, it is mandatory to have a rather detailed understanding of the wide spectrum of wave propagation phenomena involved.

In this condensed course we shall endeavour to offer a unified set of theoretical expressions based on simple first principle physics. The aim is to present theoretical expressions which lend themselves to further analysis, so as to form the basis for adaptive manipulations, and thus maximize system performance. These lecture notes are intended for advanced students or scientists with good all-round knowledge in the field of electromagnetics and wave propagation theory, but it does not assume previous acquaintance with this specialities. An effort has been made to use simple first principle first order mathematics so as to produce a set of notes which can be read from cover to cover without supporting literature. With this in mind, the first portion of the course includes wave propagation phenomena which cannot be classified as scattering and diffraction but which form a useful basis for the subsequent treatment of these more complex problems.

2 SCATTERING OF ELECTROMAGNETIC WAVES. A SUMMARY OF BASIC THEORY

Consider a volume dv within which the permittivity ε and/or the field strength $\vec{E}_o$ varies. For a plane wave incident on the scattering volume, we have

$$E_o = E_1 e^{j(\omega t - \vec{k}_1 \cdot \vec{x})}$$

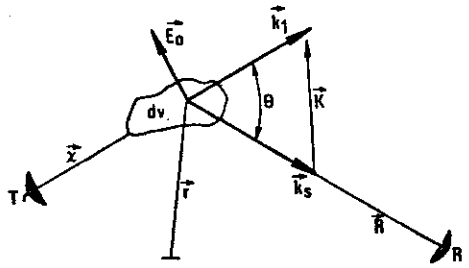

Figure 2.1 Scattering from an elementary scattering element

where $\vec{k}_1$ as shown in Figure 2.1 is the wavenumber of the incident wave.

If then $\vec{k}_s$ be the wavenumber of the scattered wave and θ be the scattering angle (angle between $\vec{k}_1$ and $\vec{k}_s$) we can define a difference wave vector

$$\vec{K} = \vec{k}_1 - \vec{k}_s$$

such that

$$|\vec{K}| = \frac{4\pi}{\lambda} \sin \theta/2$$

which is the Bragg conditions for scattering in the direction θ. λ is the wavelength of the radio wave.

If then the permittivity ε or the field strength $\vec{E}_0$ within the elementary scattering volume dv differs from the average values of ε and $\vec{E}$, a dipole moment is set up

$$d\vec{P} = \Delta\varepsilon \, dv \, \vec{E}_0$$

$$= \Delta\varepsilon \, dv \, \vec{E}_1 \, e^{j(\omega t - \vec{k}_1 \cdot \vec{x})}$$

At the distance $\vec{R}$ from this dipol moment we will have a polarization potential $\vec{\pi}$ given by

$$d\vec{\pi} = \frac{\Delta\varepsilon \, dv \, \vec{E}_0}{\varepsilon \, 4\pi \, R} e^{j(\omega t - \vec{k}_1 \cdot \vec{x} - \vec{k}_s \cdot \vec{R})}$$

Integrating this over all contributions to the polarization potential within the total volume V illuminated by the transmitter and seen by the receiver (the scattering volume). we have

$$\vec{\pi} = \frac{1}{4\pi R} \int f_\varepsilon(\vec{r}) \, \vec{E}_1(\vec{r}) \, e^{j(\omega t - \vec{K} \cdot \vec{r})} \, dr$$

where $\vec{r}$ is a position vector such that

$$\vec{k}_1 \cdot \vec{x} + \vec{k}_s \cdot \vec{R} = \vec{K} \cdot \vec{r}$$

where

$$\vec{K} = \vec{k}_1 - \vec{k}_s$$

Knowing the polarization potential $\vec{\pi}$ we can calculate the field strength $\vec{E}_s$ from the well known relationship

$$\vec{E}_s = \nabla\nabla \cdot \vec{\pi} + \vec{k}^2 \vec{\pi}$$

Provided now the scattering volume (spatial region illuminated by the radar) is small in comparison with the distance R ($R >> V^{1/3}$), then

$$k^2 \vec{\Pi} >> \nabla\nabla \cdot \vec{\Pi}$$

such that the scattered field $\vec{E}_s$ is given by

$$\vec{E}_s = k^2 \vec{\Pi}$$

The scattered field resulting from an integral of elementary scattering elements is then given by

$$\vec{E}_s = \frac{k_s^2}{4\pi R} \int_V \vec{E}(\vec{r})\ \epsilon(\vec{r})\ e^{-j\vec{K}\cdot\vec{r}}\ d^3\vec{r} \qquad (2.1)$$

omitting the time factor $e^{j\omega t}$.

Here

$\vec{K} = \vec{k}_o - \vec{k}_s$

$\vec{k}_o$ = wavenumber of incident field

$\vec{k}_s$ = wavenumber of scattered field.

Thus, if θ be the scattering angle (angle between $\vec{k}_s$ and $\vec{k}_o$) we have

$$|\vec{K}| = \frac{4\pi}{\lambda} \sin \theta/2$$

λ being the wavelength of the electromagnetic wave.

Note that equation (2.1), which is derived from Maxwell's equations, is perfectly general and does not consider the nature of the scattering object.

The $E(\vec{r})$ and $\epsilon(\vec{r})$ functions may be stochastic, in which case statistical descriptions have to be used (spatial autocorrelation functions, spatial spectra), or we may be dealing with ordered variations in which case well-behaved analytical functions may be used (1, 4, 5, 6, 7).

2.1 Correlation properties of electromagnetic waves having different frequency (bandwidth considerations)

Let us now simplify our approach and direct our attention to a one-dimensional scattering object. We combine the various factors contributing to the scattered field into one, namely one which is directly related to the scattering cross-section as a function of distance.

We define the function $f(z)$ as the delay function. This has dimension field strength such that the scattering cross-section as a function of distance z along the direction of propagation (z is measured along the direction of $\vec{K}$) is obtained by squaring the $f(z)$ function. From equation (2.1) above, we therefore have

$$\vec{E}_s(\vec{K}) = \int f(\vec{z})\ e^{-j\vec{K}\cdot\vec{z}}\ d\vec{z} \qquad (2.2)$$

$$K = \frac{2\omega}{c}$$

Note that the delay function $f(z)$ tells us how the scatterers are distributed along the direction of propagation. Using the terminology of the communication engineer, we wish to calculate the "bandwidth" of the reflecting object. The question which we ask is the following: If we illuminate an object which is characterized by a delay function $f(\vec{z})$ with a set of coherent (mutually correlated) electromagnetic waves, how are the coherence properties of the scattered wave influenced by the shape of the scattering object (by the delay function $f(\vec{z})$)?

Let us start with the general expression for the scattered field (equation 2.2 above)

$$E(K) \;-\; V\left(\frac{\omega}{c}\right) \;-\; \int f(z)\; e^{-jK\cdot z}\, dz \qquad (2.3)$$

This equation states that the field strength/voltage at frequency ω (the amplitude spectrum) is the Fourier transform of the delay function $f(z)$.

A convenient way of expressing the degree of coherence (the bandwidth properties) between different waves is by the correlation $R(\Delta\omega)$ between their complex amplitudes.

$$R(\Delta\omega) \;=\; \frac{\overline{E(\omega)\; E^{*}(\omega + \Delta\omega)}}{\overline{|E(\omega)|^{2}}}$$

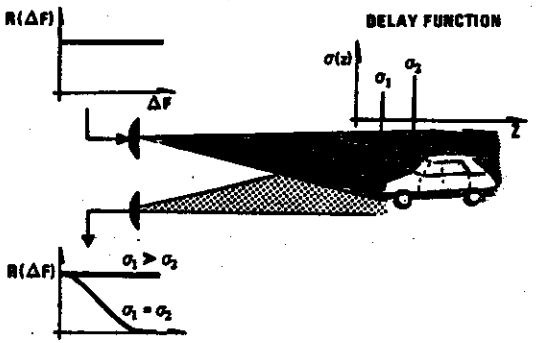

Figure 2.2 Illuminating an object with a set of correlated radio waves, the coherence properties of the scattered waves are determined by the distribution in depth $f(z)$ of the scatterers constituting the scattering object

The overbar denotes statistical average. The average may be a time average or an ensemble average.

Hence

$$\overline{E^{*}(\vec{K})E(\vec{K}+\Delta\vec{K})} \;-\; \int f(\vec{z})e^{j\vec{K}\cdot\vec{z}}\, d\vec{z}$$

$$\times \int f(\vec{z}+\vec{r})e^{-j(\vec{K}+\Delta\vec{K})(\vec{z}+\vec{r})}\, d\vec{r}$$

i e

$$\overline{E^{*}(\vec{K})E(\vec{K}+\Delta\vec{K})} \;-\; \iint e^{-j(\vec{K}+\Delta\vec{K})\cdot\vec{r}}\, d\vec{r}\; \overline{f(\vec{z})f(\vec{z}+r)}\; e^{-j\Delta\vec{K}\cdot\vec{z}}\, d\vec{z}$$

(2.4)

Note that such a statistical average can be obtained in several ways. We can select the product $E(\omega)\; E^{*}(\omega+\Delta\omega)$ for a given $\Delta\omega$ at n different values of ω and thus obtain an ensemble of n independant samples provided $E(\omega_1)$ is uncorrelated with $E(\omega_2)$ etc (see later).

Alternatively, if we are dealing with an object which is time variable (e g the sea surface), we can make use of a time average.

The second factor of Eq (2.4) is recognized as the complex autocorrelation function of the delay function. The phase-factor of the autocorrelation function (the term $e^{-j\Delta\vec{K}\cdot\vec{z}}$) is rapidly oscillating with $\Delta\vec{K}$ since the space coordinate $\vec{z}$ (the distance from the illuminator to the scattering object) is large in comparison with the incremental range $\vec{r}$.

Expression (2.4) then reduces to:

$$\overline{E(\vec{K})\ E^*(\vec{K}+\Delta\vec{K})} \sim e^{-j\Delta\vec{K}\cdot\vec{z}} \int R(\vec{r})\ e^{-j(\vec{K}+\Delta\vec{K})\cdot\vec{r}}\ d\vec{r} \qquad (2.5)$$

provided z, the distance from the radar to the object, is large in comparison with the size of the object and provided the "beat-wavelength" (see figure 2.4 and 2.5) $\frac{2\pi}{\Delta K}$ also is large in comparison with the size of the object.

Hence

$$R(\tfrac{\Delta\omega}{c}) = \frac{\overline{E(\frac{\omega}{c})\ E^*(\frac{\omega+\Delta\omega}{c})}}{A}$$

$$= \frac{e^{-j\frac{\Delta\omega}{c}z} \int R(r)\ e^{-j\frac{1}{c}(\omega+\Delta\omega)\cdot r}\ dr}{A} \qquad (2.6)$$

where A is a normalizing factor of the form $\int R(r)\ dr$.

Equation (2.6) states that the complex correlation in the frequency domain of waves scattered back from an object characterized by a given delay function is the Fourier transform of the autocorrelation function $R(r)$ of this delay function. By measuring the bandwidth of a reflecting object, we obtain directly statistical information about the delay function characterizing the object.

The modulus of the autocorrelation function $R(\frac{\Delta\omega}{c})$ is directly the Fourier transform of the $R(r)$ function. This is depicted in figures 2.2 and 2.4.

Let us now, in order to ensure a physical understanding of the general principles involved, calculate the bandwidth for a set of objects characterized by simple analytical delay functions.

First, let us consider an object which can be characterized by an exponential delay function

$$f(t) = e^{-\alpha t}$$

The $1/e$ width of this delay function is

$$t_o = \frac{1}{\alpha}$$

The voltage at frequency ω is the Fourier transform of this exponential delay function. Hence, omitting a constant:

$$V_1(\omega) = (\alpha + j\omega)^{-1}$$

Similarly, the voltage V_2 at frequency $(\omega + \Delta\omega)$ is given by

$$V_2(\omega + \Delta\omega) = \{\alpha + j(\omega + \Delta\omega)\}^{-1}$$

The normalized complex autocorrelation of these voltages is then given by

$$R(\Delta\omega) = \frac{\int_{-\infty}^{\infty} (\alpha + j\omega)^{-1}\{\alpha - j(\omega + \Delta\omega)\}^{-1}\ d\omega}{\int_{-\infty}^{\infty} (\alpha^2 + \omega^2)^{-1}\ d\omega} \qquad (2.7)$$

Solving this integral, we derive the following expression for the modulus of the autocorrelation function:

$$R(\Delta\omega) = \sqrt{1 + (\tfrac{\Delta\omega}{2\alpha})^2} \qquad (2.8)$$

To conform with the nomoclature of the communications engineer, let us, on the basis of equation (2.3) above, calculate the power spectrum and through this the "bandwidth" in the conventional manner.

Inserting $\Delta\omega = 0$ into equation (2.6) above, we obtain the following expression for the "power spectrum"

$$W(\tfrac{\omega}{c}) = \overline{E(\tfrac{\omega}{c})\, E^*(\tfrac{\omega}{c})} - \int R(r)\, e^{-j\frac{\omega}{c}r}\, dr \qquad (2.9)$$

DISTRIBUTION IN DEPTH OF SCATTERERS	FREQUENCY DEPENDANCE OF REFLECTING SURFACE	HALF POWER BANDWIDTH
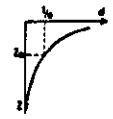 EXPONENTIAL	$W(\omega) = \frac{\sigma_o^2}{(\frac{c}{z_o})^2 + \omega^2}$	$\Delta F_{1/2} = 0.16\,\frac{c}{z_o}$ Hz
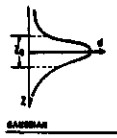 GAUSSIAN	$W(\omega) = \frac{\pi}{4}\frac{\sigma_o^2}{(\frac{c}{z_o})^2} e^{-\frac{\omega^2 z_o^2}{8c^2}}$	$\Delta F_{1/2} = 0.37\,\frac{c}{z_o}$ Hz
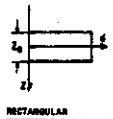 RECTANGULAR	$W(\omega) = 4\sigma_o^2 (\frac{\sin\frac{z_o}{2c}\omega}{\omega})^2$	$\Delta F_{1/2} = 0.44\,\frac{c}{z_o}$ Hz
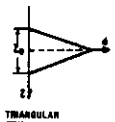 TRIANGULAR	$W(\omega) = \frac{64\,\sigma_o^2}{(\frac{z_o}{c})^2}(\frac{\sin\frac{z_o}{4c}\omega}{\omega})^4$	$\Delta F_{1/2} = 0.64\,\frac{c}{z_o}$ Hz
 DISCRETE SCATTERING CENTERS	$W(\omega) = 4\sigma_o^2 (\cos\frac{z_o}{2c}\omega)^2$	$\Delta F_{1/2} = 0.25\,\frac{c}{z_o}$ Hz

Table 2.1 The bandwidth properties (multi-frequency-radar signature) of some object classes expressed analytically

where as before $R(r)$ is the autocorrelation of the delay function $f(z)$.

Table 2.1 gives the power spectrum and also the bandwidth of a set of scattering surfaces having delay functions which are simple analytical functions.

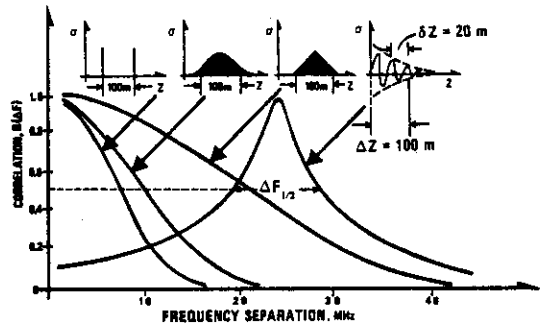

Figure 2.3 Knowing the geometrical shape of a surface (spatial distribution of scatterers) we can calculate the radar signature. If the surface manifests itself as a limited number of discrete scattering centers, the bandwidth function will be the sum of cosinus relationships as illustrated in the figure

Figure 2.3 shows the frequency correlation function in a normalized form of some scattering objects, all of size 100 m. Note the marked influence of object shape. Note also that if the object has a periodic structure such as an exponentially damped sinusoidal variation, then the correlation function in the frequency domain peaks up at a frequency separation ΔF which is different from zero and determined by the period δz:

$$\Delta F = \frac{c}{2\delta z}$$

Note also that the width of the "bandwidth function" is determined by the degree to which the sinusoidal object is damped (truncated). From simple convolution considerations we know that if a sinusoidal function is exponentially damped such that Δz is the 1/e width of the damping function, then the width of the $R(\Delta F)$ function corresponding to $R(\Delta F) = 1/2$ is given by

$$\Delta F_{\frac{1}{2}} = 0.16 \frac{c}{\Delta z}$$

If, therefore, the scattering object is the sea-surface with wavelength δz (see chapter 5.1), and if the illuminator gives an exponential intensity distribution over the spot-size Δz, then the relative wavelength resolution is given by

$$\frac{\Delta F_{\frac{1}{2}}}{\Delta F_o} = \frac{0.16 \frac{c}{\Delta z}}{\frac{c}{2\delta z}} = 0.32 \frac{\delta z}{\Delta z} \qquad (2.10)$$

Hence, if we, as an example, illuminate a sea-surface area containing 10 ocean wavelengths, then our wavelength resolution is 3%.

To ensure a thorough mathematical and physical understanding of the factors involved, we shall dwell for a moment on equation (2.9), table 2.1 and figure 2.3.

We have seen that the autocorrelation function in the frequency domain of the signal scattered back from a rough surface (rough in terms of carrier frequency wavelength) is the Fourier transform of the autocorrelation function of the delay function, whereas the amplitude spectrum of the scattered field is the Fourier transform of the delay function itself.

From general Fourier analysis (6) and also from equation (2.6) above, we know that if we Fourier transform a non-symmetrical function, a complex correlation function results. Thus, if the object is at distance z_o, as illustrated in figure 2.4, the delay function will be non-symmetrical and the autocorrelation function $R(\Delta F)$ will oscillate with period $\frac{c}{2z_o}$. The envelope of the correlation function $R(\Delta F)$ is obtained by taking the modulus of the complex autocorrelation function as in equation (2.6) above.

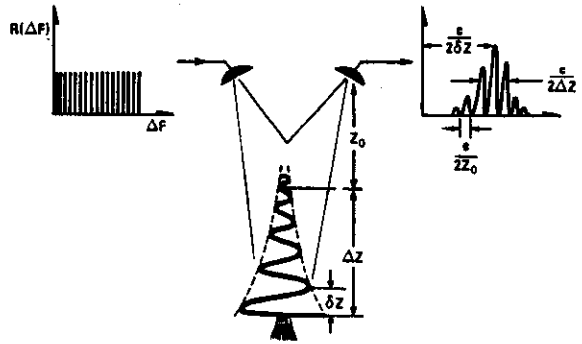

Figure 2.4 Illuminating the object with a set of electromagnetic waves with different frequencies, the correlation function in the frequency domain of the reflected wave gives information about the distance to the object, the size of the object, and its shape

Thus, by measuring the complex autocorrelation function in the frequency domain, obtained by using a multifrequency radar system, we obtain information about the distance to the object, the size of the object and about its shape. Physically this mathematical statement can be visualized from figure 2.5 (7).

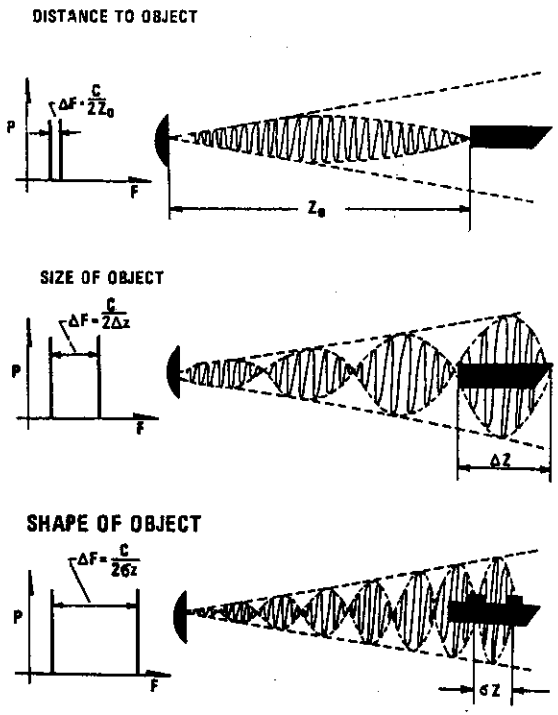

Figure 2.5 The distance to the object z_o is determined by transmitting two microwave frequencies with spacing $\frac{c}{2z_o}$, the size of the object is obtained in the same manner by transmitting two frequencies with spacing $\frac{c}{2\Delta z}$. Finally, the shape is obtained by transmitting waves with the larger frequency separation $\frac{c}{2\delta z}$ (ref 7)

To measure the distance to the object (assumed large in comparison with the size of the object) we transmit two microwave frequencies and we adjust their frequency separation so as to obtain one spatial beat period between transmitter and target. In practice, what this means is the following. Assume that one is interested in knowing when an approaching

object passes the 100 km distance zone. Disregarding for the moment Doppler phenomena (see later) we shall transmit two radar frequencies with mutual separation $\Delta F = \frac{c}{2z_o} = 1.5$ kHz. If, as an example, the length of this object at 100 km range should be 100 m long, to be of interest, then we should check if the two transmitted frequencies with mutual spacing $\Delta F = \frac{c}{2\Delta z}$ where $\Delta z = 100$ m are in phase when scattered back from the target. This calls for two frequencies with mutual spacing 0.48 MHz. Note that the carrier frequency only enters into the question in as much as it influences the scattering cross-section of the target.

2.2 Correlation properties of scattered electromagnetic field in space, angular distribution

We have completed the section on the correlation properties of electromagnetic waves having different frequency. We have seen that by measuring the degree to which waves having different frequency are correlated, we obtain information about the longitudinal distribution of the scatterers. If we are dealing with a thin reflector (zero distribution in depths), then the bandwidth of the reflector is very large. Conversely, if the scatterers are distributed over a large region in space, the bandwidth is small.

We shall now focus the attention on the transverse distribution of the scattering elements constituting the scattering object. In order to reveal this transverse structure, we shall use another characteristic property of electromagnetic waves, namely, its spatial correlation properties. We shall illuminate the scattering object with one single frequency, and at the receiving site we shall make use of a set of antenna elements distributed along a base-line or in a plane which is perpendicular to the line joining the receiving array and the scattering object. At each element, we shall measure the amplitude and the phase of the impinging wave. On the basis of these point-observations of fieldstrength, information about the target can be extracted. This will be the subject of the current section.

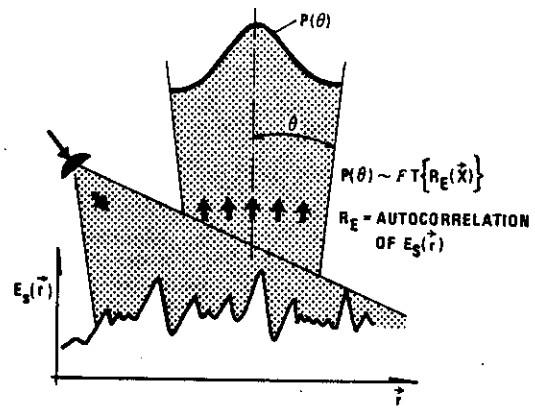

Figure 2.6 The geometry of the backscattering process. The illuminating field gives rise to a scattered fieldstrength distribution $\vec{E}_s(x)$

First, consider figure 2.6 illustrating the scattering process. We illuminate a surface with a single wave. Depending on the properties of the surface, we obtain a certain fieldstrength distribution of the scattered field $\vec{E}_s(x)$.

We shall now calculate the angular distribution $P(\theta)$ of the waves scattered from this surface. From eq (2.1) above, we find the following expression for the scattered field in terms of the fieldstrength distribution over the scattering surface:

$$\vec{E}_s(\vec{K}) \sim \int \vec{E}(\vec{x})\, e^{-j\vec{K}\cdot\vec{x}}\, d\vec{x} \qquad (2.11)$$

Since

$$K = \frac{4\pi}{\lambda} \sin \frac{\theta}{2}$$

this equation tells us how the scattered field is distributed in direction θ. From this we shall derive the angular power distribution $P(K)$ as follows:

$$P(\vec{K}) \sim E_s(\vec{K})\, E_s^*(\vec{K})$$

$$\sim \iint E^*(\vec{x})\, E(\vec{x}+\vec{r})\, e^{j\vec{K}\cdot\vec{x}}\, e^{-jK(\vec{x}+\vec{r})}\, d^3\vec{x}\, d^3\vec{r}$$

$$\sim \int d^3\vec{r}\, e^{-j\vec{K}\cdot\vec{r}} \int d^3\vec{x} E(\vec{x})\, E(\vec{x}+\vec{r}) \qquad (2.12)$$

The second integral is immediately recognized as the spatial autocorrelation $R_E(\vec{r})$ of the fieldstrength distribution.

Hence

$$P(\vec{K}) \sim P(\sin\theta) \sim \int R_E(\vec{r})\, e^{-j\vec{K}\cdot\vec{r}}\, d^3\vec{r} \qquad (2.13)$$

This equation tells us that the angular spectrum (radiation pattern) of the scattered wave is the Fourier transform of the fieldstrength distribution over the scattering region when this distribution is expressed statistically in terms of its spatial autocorrelation.

This is a relationship which is very well known from antenna theory: The radiation pattern (angular power distribution) of an antenna with aperture A is obtained by the Fourier transform of the fieldstrength distribution over this aperture. Thus, if our $E(\vec{x})$ function is a rectangular one, implying that the fieldstrength is evenly distributed over the antenna aperture, then the angular power distribution is of the form $\frac{\sin\theta}{\theta}$ and the beamwidth $\beta = \frac{\lambda}{D}$ where D is the aperture

size. Conversely, if the fieldstrength distribution over the aperture is of the $\frac{\sin x}{x}$ form, then the angular distribution of the scattered wave is a rectangular one.

We shall be using these simple relationships extensively in the subsequent sections.

Now let us return to eq (2.13) above, and use this as the basis for studying another important property of the scattered field, namely the spatial correlation of field-strength.

In the discussion which we have just completed, we considered the case of a "transmitting antenna".

Now let us consider the case of a receiving one. Our receiving antenna consists of a set of antenna array elements which permits us to measure amplitude and phase at each array element. The power reaching this array antenna is distributed as $P(\theta)$ over an angular region. Applying the inverse Fourier transform of eq (2.13) above, it is intuitively obvious that we obtain information about the spatial correlation properties of the fieldstrength:

$$R_E(\vec{r}) \sim \int P(\vec{K})\, e^{j\vec{K}\cdot\vec{r}}\, d\vec{K} \qquad (2.14)$$

This equation tells us that the spatial correlation of the scattered field is the Fourier transform of the angular power distribution.

We see from this figure that if we are to resolve an object of transverse extent Δx by means of a receiving antenna array at distance R from the object, we shall have to measure the fieldstrength distribution over a spatial region $L_x = \frac{R\lambda}{\Delta x}$.

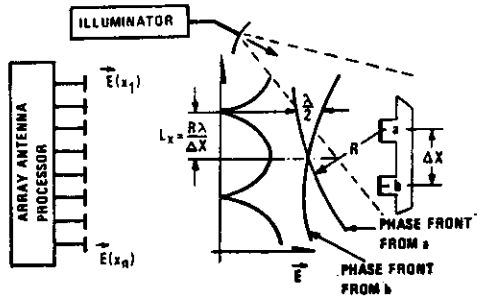

Figure 2.7 Transverse distribution of fieldstrength. The spatial autocorrelation of fieldstrength is the Fourier transform of the angular power spectrum. The size (width) Δx of the object manifests itself as a "transverse interferogram"

Summing up these findings, we should note that by measuring the fieldstrength distribution across a broadside array (amplitude and phase at each array-point), we obtain direct information about the transverse scattering properties of the scattering object.

It takes little imagination to see the analogy between this spatial autocorrelation function and the autocorrelation function in the frequency domain discussed above. In the multi-frequency case, we can "filter out" certain longitudinal spatial distributions of the scattering object by using frequency filters. In the case of the broadside array, we can "filter out" certain transverse properties of the scattering

elements by providing a "spatial filter". This means that we can make an adaptive system by adjusting the amplitude and phase of the receiving antenna elements so as to match the wavefront of the wave system which is reflected back from the target of interest, whereas the waves originating from the terrestrial background against which the target is viewed can be suppressed. Such adaptive phased array systems have been the subject of any recent contributions (ref 8, 9). In this chapter we shall limit ourselves to referring to figure 2.7 where a symbolic presentation of the phased array concepts are given. We shall also point out the very striking analogy between the multi-frequency adaptive system and that involving phased arrays.

2.3 Temporal correlation properties of a scattered wave, (motion pattern considerations, Doppler)

We have shown that if a rigid body is illuminated by a set of electromagnetic waves having different frequencies, information about the distribution in depth (along the direction of wave propagation) is obtained by studying the correlation properties of the scattered waves. Specifically, if two electromagnetic waves with frequency separation ΔF are illuminating the object, we obtain information about a particular irregularity scale L (spatial spectrum component $K = \frac{2\pi}{L}$) where L is related to frequency separation ΔF, as follows:

$$L = \frac{c}{2\Delta F}$$

Let us now assume that a rigid body characterized by the delay function $f(z)$ (distribution in depth of the scattering elements) is moving with velocity $\vec{V}$. We now want information about the Doppler shift which this frequency ΔF is subjected to.

We base this calculation on the basic Doppler equation

$$f = \frac{1}{2\pi} \vec{K} \cdot \vec{V} \qquad (2.15)$$

Here $K = \frac{2\pi}{L}$, where L is the scale-size to which the frequency pair ΔF is matched. The Doppler shift associated with the difference frequency ΔF is therefore:

$$f = \frac{1}{2\pi} \vec{K} \cdot \vec{V} = \frac{1}{2\pi} \frac{2\pi}{L} V \cos \phi$$

$$= \frac{2\Delta F}{c} V \cos \phi \qquad (2.16)$$

where ϕ is the angle between the wave vector $\vec{K}$ and the velocity vector $\vec{V}$.

Hence, if we illuminate a moving object with two electromagnetic waves with frequency spacing ΔF (coupled to scale size $L = \frac{c}{2\Delta F}$), this frequency ΔF is subjected to a Doppler shift f which is proportional to ΔF and to the velocity V of the object. The power associated with the Doppler frequency f is the same as that associated with the frequency ΔF and expressed by equation (2.9).

Thus, knowing the shape of the target (see figure 2.3), and its velocity, the Doppler spectrum can be calculated on the basis of equations (2.9) and (2.16).

Then let us consider a flexible object. The spectrum of irregularity scales constituting the scattering body are moving at different velocities. Consider one particular such scale L which is distributed throughout the scattering body. Let us assume that the width of the velocity distribution of the scattering elements characterized by the scale L (Fourier component $K = \frac{2\pi}{L}$) is δV. This velocity distribution will, obviously, give rise to a Doppler spectrum the width of which is determined by the velocity spread:

$$\Delta f = \frac{1}{2\pi} \vec{K} \cdot \delta\vec{V} \qquad (2.17)$$

In terms of the illuminating frequency ΔF, we get the following expression for Doppler broadening

$$\Delta f = \frac{2\Delta F}{c} \delta V \cos \phi \qquad (2.18)$$

Figure 3.5 shows the Doppler shift which each radio frequency separation ΔF is subjected to, when the scattering object is a rigid ship characterized by two scattering centers 100 m apart moving at a velocity of 20 knots.

Now let us finally consider the case where the scatterers are distributed over the entire area illuminated by the radar beam. If the beamwidth is β, then the direction of the backscattered radio wave will vary between $-\beta/2$ and $+\beta/2$, such that the direction of the wave vector $\vec{K}$ will vary over the angle β.

As seen from the basic Doppler equation above, this variation in $\vec{K}$ will lead to a Doppler spread in excess of that caused by the velocity spread δV.

Let us assume that the scatterers are filling the radar beamwidth and that they are moving at speed V_c along a direction which is normal to the center line of the radar beam. Scatterers located at the center line obviously give rise to no Doppler shift whereas scattering elements located at extreme positions give a Doppler shift

$$\Delta f = \pm \frac{2\Delta F \, V_c}{c} \sin \beta/2$$

as seen from equation (2.16) above. For narrow antenna beams, therefore, the Doppler broadening caused by a cross beam drift velocity V_c of the scattering elements is given by (ref 10):

$$\Delta f = \frac{2\Delta F}{c} V_c \cdot \beta \qquad (2.19)$$

This Doppler broadening effect is in practice of little importance when dealing with targets of finite size, but it may be significant when dealing with a strong cross-beam ocean surface current.

3 FUNDAMENTALS OF RADIO WAVE PROPAGATION THROUGH THE ATMOSPHERE

It is the purpose of the following section to analyze a set of practical propagation media with a view to obtaining analytical expressions providing information about

- pathloss
- bandwidth (resolution capability longitudinally)
- spatial coherence (resolution capability transversely)

We shall endavour to offer a unified set of theoretical expressions based on simple first principle physics. The aim is to present theoretical expressions which lend themselves to further analyses, so as to form the basis for adaptive manipulations, and thus maximize system performance. Furthermore, we shall base our theoretical approach on the concepts derived in section 2 above, where we presented the basic theory for scattering/diffraction.

Ideally, in the case of a radar system, we would like to organize ourselves, so as to first measure the properties of the propagation medium, then the characteristics of the target background, and finally, knowing in advance the signature of the target, we could optimize the total system performance. This is illustrated in the form of an artist's conception in Figure 3.1.

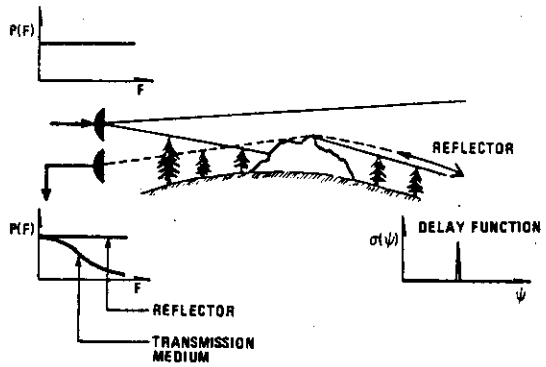

Figure 3.1 Limitations of radar performance imposed by the propagation medium. Having "test-targets" to our disposal, we can assess the influence of the intervening propagation medium

3.1 Line-of-sight propagation

Figure 3.2 shows the distance dependence of a radio field for various propagation mechanisms. Within line-of-site, the power density decreases with distance as R^2 and in terms of transmitted power P_T, gain of transmitting antenna G_T, area of receiving aperture A, and distance between transmitter and receiver R the received power P_R is given by:

$$\frac{P_R}{P_T} = \frac{G}{4\pi R^2} A \qquad (3.1)$$

The received power decreases gradually as the distances increases, for a given power and beam configurations there is no parameter which can be altered in order to improve the situation.

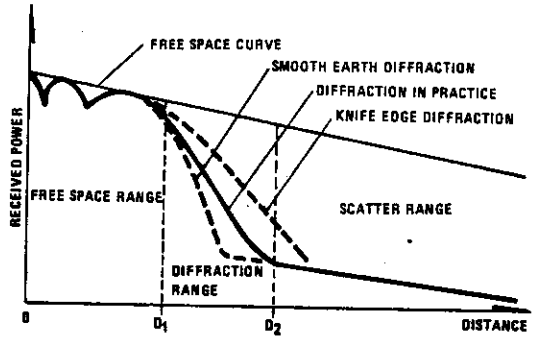

Figure 3.2 Factors determining the path loss in tropospheric propagation

Then let us consider what happens if part of the transmitted energy is illuminating the ground surface and reflected into the direct wave. If now H_T is the height above the reflecting surface of the transmitting antenna, and H_R is the corresponding height of the receiving antenna, then the difference in pathlength of the direct wave relative to that of the reflected wave, is given by

$$\Delta = \frac{2H_T H_R}{R}$$

Phase angle Φ between the two waves is therefore

$$\Phi = \frac{4\pi H_T H_R}{\lambda R}$$

Such that when $\phi = \pi$ the two waves appear in antiphase giving rise to a minimum in the plot of received power versus distance, as shown in Figure 3.2. Similarly, if the phase angle is equal to 2π, we have constructive interference and we get a maximum. Accordingly, in order to change a maximum to a minimum without altering the geometry i e the position of the transmitter and the receiver, the wavelength will have to be changed by a factor 2. This, obviously, is within reach in an adaptive communication system (see later).

Note that this statement is strictly correct only if we neglect the effects of surface waves. If this can not be neglected we shall have to include the surface wave in addition to the direct wave and the reflected wave. This involves adding the surface wave term

$$(1 - R)\ A\ e^{i\phi}$$

where R is the reflection coefficient of the ground and A the surface wave attenuation factor. These parameters vary both with polarization and with the electrical constants of the ground. For near grazing paths, R is approximately equal to -1 and A can be neglected if the antenna is elevated more than a wavelength above the ground (or more than 5 - 10 wavelengths above sea water). This condition is generally fulfilled in practice when dealing with microwaves.

Now let us assume that we will like to adjust the height of the receiving antenna in such a way so as to achieve constructive interference. As seen from the above expression, this is achieved by shifting the receiving antenna vertically through a distance

$$\Delta H_R = \frac{\lambda R}{4H_T} \qquad (3.2)$$

Hence, if we are dealing with a target of vertical extent ΔH_{TARGET} we shall have to controll the propagation parameters so as to ensure that $\Delta H_R \geq \Delta H_{TARGET}$.

Then let us, in terms of bandwidth, consider the properties of a propagation circuit involving ground reflections. Having already calculated the delay function related to our transmission circuit, the bandwidth is readily obtained as a function which is proportional to the inverse of delay. Specifically, if the delay function, as in our case, consists of two δ-functions with separation

$$\Delta = \frac{2H_T\ H_R}{R}$$

the correlation properties in the frequency domain of the reflected signal is given by the Fourier transform of the delay function. The Fourier transform of two δ-functions is a cosine relationship. The half power bandwidth of the first order is therefore , as we have already seen in section 2 above, given by

$$\Delta F = 0.25\ \frac{c}{\Delta} \qquad (3.3)$$

Introducing the geometrical expression for Δ above, we find that the bandwidth is given by

$$\Delta F = \frac{c \cdot R}{8H_T\ H_R} \qquad (3.4)$$

The simple formulas above are based on the assumption that radio rays propagate along stright lines. If the atmosphere is not homogeneous as regards refractive index, this is not the case. If we are dealing with a vertical profile of refrative index we shall experience bending (refraction).

Knowing the refractive index profile we can calculate the ray bending from Snell's law. We are thus able to calculate the total bending to which a ray is subjected when propagating from the radar to the target (and back along the same path). This bending is dependent on the initial direction ϕ of the ray relative to the isosurface of refractive index (11). In this simple treatment we shall limit ourselves to near horizontal directions of the radar beam.

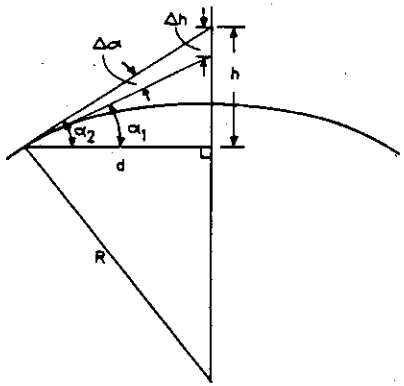

Figure 3.3 Geometry related to height errors caused by refraction

From this simple geometry shown in Figure 3.3, then, we have the following geometrical relationships:

$$\frac{1}{a} = \frac{1}{R} + \frac{dn}{dz} \cos \phi \qquad (3.5)$$

$$a = k R$$

$$K = \frac{1}{1 + R \frac{dn}{dz} \cos \phi} \qquad (3.6)$$

Direction to target for the case of no ray bending is given by

$$\alpha_o = \frac{d}{R}$$

R being the real earth's radius.

Similarly, with a bending corresponding to an effective earth's radius "a" the ray direction is

$$\alpha_1 = \frac{d}{a}$$

$$\text{i e} \quad \frac{\Delta h}{h} = \frac{(\alpha_o - \alpha_1) d}{\alpha_1 d}$$

and

$$\frac{\Delta h}{h} = \frac{\alpha_o}{\alpha_1} - 1 = (k - 1) \qquad (3.7)$$

where k is the ratio of effective earth's radius to real radius.

Figure 3.4 shows a practical example of the probability distribution of the bending parameter α/R. These were obtained from conventional routine meteorological radio sondes released from Sola, Norway, during the winter of 1965.

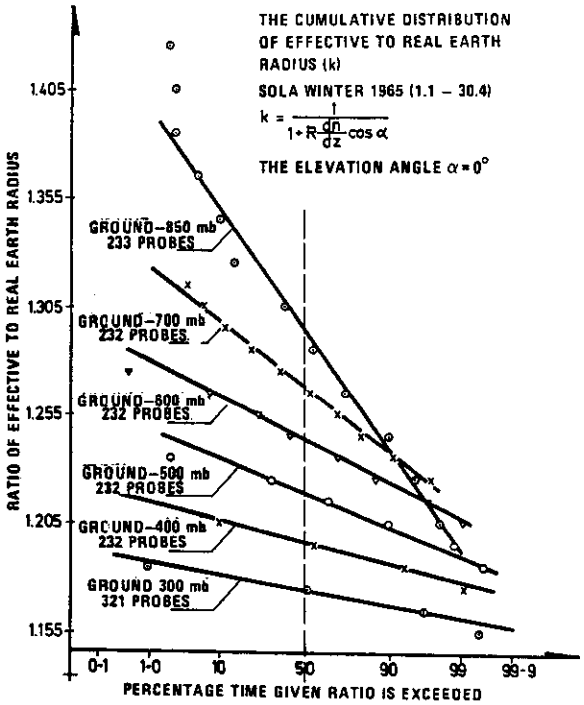

Figure 3.4 Probability distribution of the ratio of effective to real earth radius calculated by the aid of data from routine meteorological radio sondes

Based on the probability distribution of the effective to real earth radius, the total bending (height error) can be calculated.

These are shown in Figure 3.5 for zero elevation angle.

For the sake of illustrating the severity of height errors, numbers are given for the specific case of a target at a height of 1500 meters.

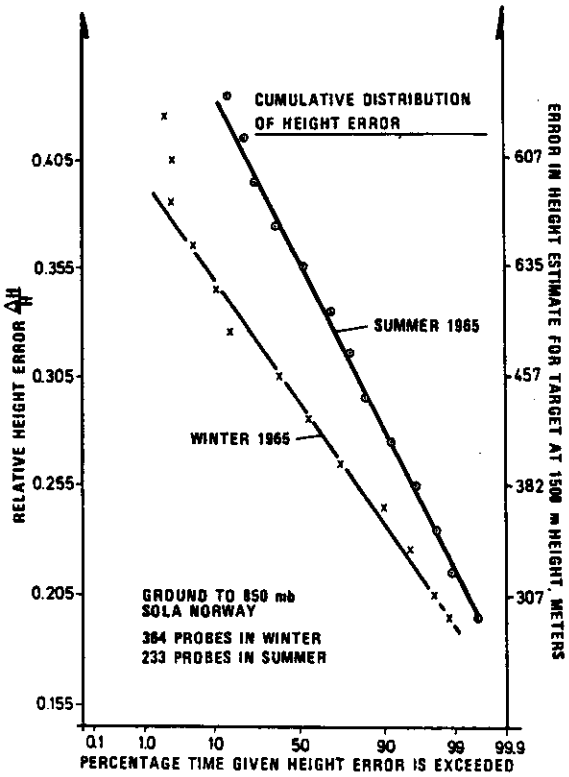

Figure 3.5 Probability distribution of height error calculated on the basis of radiosonde information as presented in Figure 3.4 above

So far we have restricted the discussion to the case where the spatial small scale fluctuations in refractivity were negligible, we shall thus experience refraction only and no scattering. We shall no consider an atmosphere which is characterized by small scale spatial refractivity fluctuations and the effect of these on line-of-sight propagation.

As a consequence of the fact that irregularities in the atmospheric refractive index structure lead to multipath phenomena and delay variations when an electromagnetic wave passes through the irregular transmission medium, we suffer a loss in bandwidth. We shall now give some theoretical results, which are well confirmed experimentally, giving information about the amplitude covariance as a function of frequency separation (i e bandwidth properties of the medium) and as a function of spatial separation.

Before referencing the results of comprehensive calculations, we shall, as above, give some quantitative results for the purpose of ensuring a physical understanding of the basic physics involved.

Referring to the simple geometrical sketch of Figure 3.6, we see that there are two extreme paths through which the electromagnetic waves can travel from the transmitter T to the receiver R. One is the shortest direct way from T to R, the

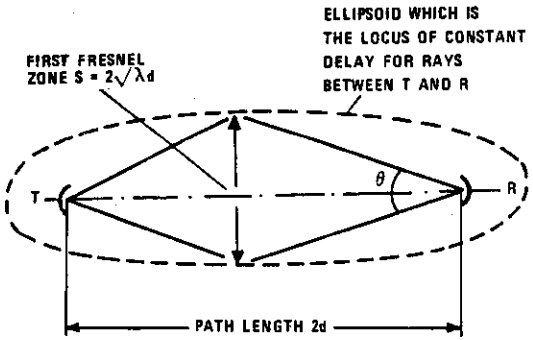

Figure 3.6 The geometry of line-of-sight propgation

the other is via a path which is half a wavelength longer than the direct route. The result of these two waves is the vector sum of two signals with a 180° difference in phase causing destructive interferences.

To the first order, therefore, we would expect the width θ of the angle of arrival spectrum at the receiving point to be given by

$$\tan^{-1}\theta = \frac{\sqrt{\lambda d}}{d}$$

$$\theta \simeq \frac{\sqrt{\lambda d}}{d} \qquad (3.8)$$

Knowing the angular power spectrum (the beamwidth), the correlation distance in a plane through the location of the receiver normal to the line T - R can be calculated. We have shown in section 2 above, that this spatial correlation of field strength is the Fourier transform of this angular power spectrum.

If this power spectrum is a $\frac{\sin x}{x}$ function, then the Fourier transform is a rectangular function. If the width of this, i e the correlation distance of field strength, be L , then we have the following relationship between the half-power width of the beam $\theta_{\frac{1}{2}}$ and the correlation distance L

$$\theta_{\frac{1}{2}} = \frac{0.88\ \lambda}{L} \qquad (3.9)$$

where λ is the wavelength of the electromagnetic wave.

In passing, note that this is the same expression as that relating antenna beamwidth $\theta_{\frac{1}{2}}$ to the antenna aperture diameter L. This is not surprising since the antenna radiation pattern (the $P(\theta)$ function) is the Fourier transform of the illuminating field strength distribution over the antenna aperture.

From equations (3.8) and (3.9) above, therefore, we have

$$\frac{0.88\ \lambda}{L} = \frac{\sqrt{\lambda d}}{d}$$

i e correlation distance $L = 0.88\ \sqrt{\lambda d}$ (3.10)

Thus, the correlation distance of field strength transverse to the line of propagation is comparable with the first Fresnel zone.

Then let us calculate the bandwidth $\Delta\omega$.

From chapter 2 above, we have learnt that the bandwidth function (autocorrelation function in the frequency domain) is obtained by Fourier transforming the delay function.

For simplicity, let us again assume that the delay function is of the $\frac{\sin x}{x}$ form with a half-power width $\Delta\tau = (\lambda/2)/C$. The bandwidth function, i e the frequency transfer function $P(\Delta F)$ or the correlation function in the frequency domain $R(\Delta F)$, would then be a rectangular function the width of which is

$$\Delta F = \frac{1}{\Delta\tau} = \frac{2C}{\lambda}$$

$$= \frac{1}{2} \text{ frequency of the electromagnetic wave} \qquad (3.11)$$

These were the approximate results. Lee and Harp (ref 12)) have performed rigorous calculations based on a general expression for the spatial distribution of refractive index. For details the reader is referred to ref (12) and also to ref (13).

Summing up this section on line-of-sight propagation mechanisms in relation to an adaptive radar (or communications) system, the following should be noted:

- The path loss can be minimized by adjusting the height of the transmitting antenna or the wavelength.
- The vertical coherence distance of fieldstrength can likewise be maximized by adjusting the antenna height. The lower the antenna height, the larger is the coherence distance.
- If we are dealing with a homogeneous refractive index structure, the bandwidth of the line of sight circuit can be optimized by decreasing the height of the transmitting antenna.
- Spatial fluctuations in refractive index resulting from atmospheric turbulence impose severe limitations on bandwidth as well as on the vertical coherence distance. There is nothing we can do in order to improve this situation, except noting that the turbulent transmission medium is very variable. Given sufficient time, there will be a time interval where conditions are very much better than the average conditions.

3.2 Propagation mechanisms involving scattering and reflection

As the demand for reliable broad band communication circuits high resolution adaptive radar systems increases, so does the need for detailed information about the transmission medium.

The multitude of new demans leads to a very versatile and sophisticated usage of the transmission medium. This, in turn, calls for a very comprehensive description of the medium. The transmission medium constitutes the limiting factor in many interesting and potentially powerful communication and radar techniques of which the following should be mentioned:

- Spread spectrum modulation systems and multi-frequency radar systems are very sensitive to frequency selective fading, i e require a large instantaneous bandwidth. Hence we shall need information about the circuit bandwidth and its variability.

- Large synchronous time division multiplex communication systems set narrow limits with regard to variations in time delay in the system. As a consequence, information about the delay spectrum and its temporal variability is mandatory.

- Environmental surveillance systems requiring a large spectrum of wavelengths to illuminate the scene of interest. To optimize system performance, we shall need detailed information about the effects of the intervening propagation medium.

With these applications particularly in mind, the current chapter will discuss scattering mechanisms and channel characterization in relation to broadband communications and multi-frequency, high resolution radar systems.

3.2.1 Basic relationships in over-the-horizon scatter propagation, a brief summing up

When discussing the characteristic properties of a scattered (or diffracted) wave in relation to radar and communication systems, it is useful to have a physical understanding of the basic principles involved.

With reference to section 2 above and earlier works (1, 10, 14) a brief sketch of some of the more important derivations will be given.

Consider a volume element $dv = dx\,dy\,dx = d^3\vec{r}$ within the scattering volume V, this scattering volume being confined to

the spatial region in the troposphere illuminated by the transmitting antenna and "seen" by the receiving antenna. If the permittivity (refractive index squared) within the elementary volume differs by an amount $\Delta\varepsilon$ from the average value of the permittivity ε_o, the element of dielectric becomes polarized, giving rise to a dipole moment $d\vec{P} = \Delta\varepsilon\, dv\, \vec{E}_o$ when under the influence of an electric field $\vec{E}_o$. At distance R from the scattering element the dipole moment results in a polarization potential $d\pi$ and provided $k^2\vec{\pi} >> \nabla\nabla\cdot\vec{\pi}$ (which requires $R >> V^{1/3}$), the scattered field strength $\vec{E}_s = k^2\vec{\pi}$, where $\vec{k}$ is the wave number of the electric field. The scattered field resulting from the integral of elementary scattering elements is then given by

$$E_s = \frac{k_s^2}{4\pi R} \int E_o(\vec{r})\ \varepsilon(\vec{r},t)\ e^{-j\vec{K}\cdot\vec{r}}\, d^2\vec{r} \qquad (3.12)$$

where $\vec{K} = \vec{k}_o - \vec{k}_s$, $\vec{k}_o$ and $\vec{k}_s$ being the wave numbers of the incident and the scattered fields, respectively, such that $|K| = (4\pi/\lambda)\sin\theta/2$, where θ, the scattering angle, is the angle between $\vec{k}_s$ and $\vec{k}_o$.

Note that (5.12), which is derived from Maxwell's equation, is perfectly general and does not consider the nature of the refractive-index irregularities described by the function $\varepsilon(\vec{r},t)$. This function may be a stochastic one, in which case the refractive-index field is conveniently described by the spatial autocorrelation function of refractive index, or we may be dealing with an ordered variation in ε, say a horizontal layer through which the refractive index varies in a systematic fashion expressible as a well-behaved function (see section 3.2.8).

In exactly the same way, $\vec{E}_o(\vec{r})$ describes the spatial variations in the electric field within the scattering volume.

From the basic equation above, we see that there are two limiting cases:

a) If the field $\vec{E}(\vec{r})$ is constant within the scattering volume (or varies slowly in space in comparison with the $\varepsilon(\vec{r})$ function), then

$$\vec{E}_s = \frac{k^2 \vec{E}}{4\pi R} \int_V \varepsilon(\vec{r})\, e^{-j\vec{K}\cdot\vec{r}}\, d^3\vec{r}$$

which states that <u>the scattered field $\vec{E}_s$ is proportional to the Fourier transform of the spatial variation in refractive index within the scattering volume V</u>.

b) If $\varepsilon(\vec{r})$ is constant within the scattering volume, then the equation tells us that <u>the diffraction field $\vec{E}_D$ is the Fourier transform of the spatial variation in field strength within the scattering volume V (see section 5.3)</u>.

$$\vec{E}_D = \frac{k^2 \varepsilon}{4\pi R} \int_V E(\vec{r})\, e^{-j\vec{K}\cdot\vec{r}}\, d^3\vec{r}$$

The intermediate conclusions are visualized in Figure 3.7 .

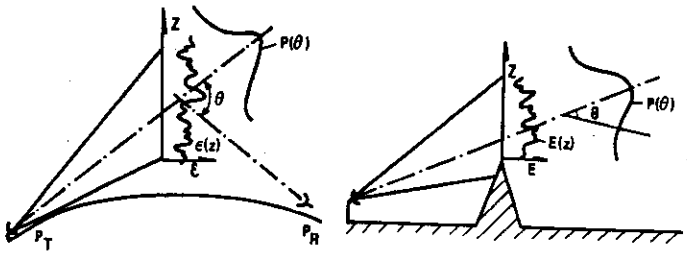

a b

Figure 3.7 a) The scatter field is the Fourier transform of the patial variations in refractive index $\varepsilon(z)$

b) The diffracted field is the Fourier transform of the spatial variation in the illuminating field $E(z)$

Now let us concentrate on the scattered field associated with spatial variations in refractive index $\varepsilon(r)$.

We shall need information about the scattered power P as a function of scattering angle θ. To obtain this we multiply $\vec{E}_s$ by its complex conjugate $\vec{E}_s^*$ obtaining the scattering cross-section σ given by

$$\sigma(\theta) = (\pi k^4/2)\, \Phi(\vec{K}) \qquad (3.13)$$

where $\Phi(\vec{K})$ is the spatial "power spectrum" of the refractive-index irregularities such that $\Phi(\vec{K})$ is the Fourier transform of the spatial autocorrelation function of $\varepsilon(\vec{r})$. The scattering cross-section σ is defined as the mean power in the scattered wave per unit power density of the incident wave in the scattering volume, per unit solid angle in the direction of $\vec{k}_s$, per unit scattering volume.

Note that the power spectrum $\Phi(\vec{K})$ is the Fourier transform of the spatial autocorrelation function of refractive index fluctuation.

Having obtained an expression for the angular power spectrum of the scattered field in terms of the function $\Phi(\vec{K})$ describing the spatial variation in refractive index, the questions which arise are the following:

- Does there exist a unique form of the $\Phi(\vec{K})$ function for the tropospheric propagation medium?
- To what extent does the $\Phi(\vec{K})$ function vary with time and with geographical location of the scattering volume?

Many forms of the $\Phi(\vec{K})$ function have been suggested. The more important ones are associated with the following names: Obukhoff-Kollmogorov, Booker-Gordon, Bolgiano, Willers-Veisskopf, Norton.

In this brief discussion of the subject, a detailed discussion of the relative merits and justification for the various $\Phi(\vec{K})$ functions does not seem justified. There is good justification (10, 15) for writing the power spectrum in the form

$$\Phi(\vec{K}) = K^{-n} \qquad (3.14)$$

where n is a number that, depending on the atmospheric conditions, may vary between approximately 2 and 7. Many theories predict $n = 11/3$. Experiments show (references 16 to 22) that n varies within wide limits. The theoretical value $n = 11/3$ appears to be close to the median value of the observations (see later).

Based on the refractive index spectrum expressed in the form $\Phi(K) = K^{-n}$ we shall now calculate some of the characteristic parameters of a long-distance forward scatter circuit. There are many such, of which should be mentioned: time-delay spectrum, bandwidth, horizontal and vertical correlation distance of field strength, antenna-to-medium coupling loss.

These will now be considered

3.2.2 Calculation of pulse distortion in terms of radio-meteorological parameters

Our task is now to calculate the delay spectrum (pulse distortion) and subsequently the bandwidth on the basis of information about the refractive index structure $\varepsilon(\vec{r})$ as expressed by its spatial power spectrum $\Phi(K)$, written in the form $\Phi(K) = K^{-n}$.

Using a wide-beam antenna so that the multipath transmission is governed by the scattering mechanism rather than by the beam geometry, we first seek an expression relating path length ℓ and the position in space of the scattering element; i e we require an expression relating ℓ and the scattering angle θ (see Figure 3.8). If d is the length of the chord between T and R, then simple geometrical calculations give the required results, namely

$$\theta = 2\left|(\ell/d)^2 - 1\right|^{\frac{1}{2}}$$

If we transmit a short radio pulse, the power that reaches the receiver has travelled through a wide spectrum of different paths.

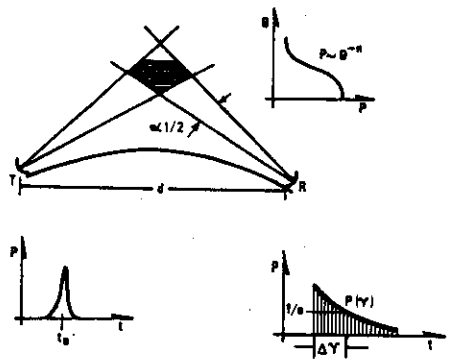

Figure 3.8 The delay spectrum is determined by the variation in path length

By substituting for θ in the expression for the angular power spectrum ($P \sim \theta^{-n}$), we get the spectrum relating power and path length. Normalizing this power with respect to the power received via the shortest propagation path ℓ, namely that determined by the earth's tangent planes, we get: $\ell_o = d\left|\ell + (d/2a)^2\right|^{\frac{1}{2}}$, (where a is the effective earth radius), the power spectrum takes the form

$$|P(\ell)/P/\ell_o)| = \left(\frac{4a^2}{d^2}\right)^{-n/2} |(\ell/d) - 1|^{-n/2}$$

Expressing this spectrum in terms of the path length $\Delta\ell$, which is in excess of the minimum path length ℓ_o (i e writing $\ell = \ell_o + \Delta\ell$), we find that the power spectrum referred to ℓ_o is given by

$$|P(\Delta\ell)/P(\ell_o)| = |1 + \left(\frac{8a^2}{d^3}\right) \Delta\ell|^{-n/2}$$

And since $\Delta\ell = \tau C$, where C is the velocity of light, the delay spectrum referred to τ_o (the shortest time delay) is given by

$$|P(\tau)/P(0)| = |1 + \left(\frac{8a^2 \tau C}{d^3}\right)|^{-n/2} \qquad (3.15)$$

The 1/e width of this delay spectrum is then given by

$$\Delta\tau = \left(\frac{d^3}{8a^2 C}\right)(e^{2/n} - 1) \qquad (3.16)$$

If, on the other hand, the antenna beams are narrow such that the spread in the path length is determined by beam geometry rather than by the $\Phi(K)$ function (i e the beams are so narrow that $\Phi(K)$ can be considered constant when θ varies within the scattering volume), then we can find a simple expression for the delay spectrum in terms of geometrical parameters. Under these conditions the delay spectrum will have a width $\Delta\ell/C$ given by (23)

$$\Delta\tau = \frac{d}{2C}\left(\frac{d}{a}\beta + \beta^2\right)$$

where β is the beamwidth.

Having expressed the delay spectrum in terms of radiometeorological parameters, we shall now apply a similar method to calculate the bandwidth of the transmission channel.

3.2.3 Calculation of bandwidth

To avoid the confusion which often arises when the term "bandwidth" is used in relation to scattering processes, let us define what we mean with bandwidth.

Consider the case where several radio waves having different frequencies are transmitted simultaneously. At the receiver the power at each of these frequencies is measured as a function of time (i e we measure $P_{F_1}(t)$, $P_{F_2}(t)$ etc). If we take the instantaneous ratio of power at the various frequencies and integrate the ratio (i e we form $\int \frac{P_{F_1}(t)}{P_{F_2}(t)}\,dt$) then we get information about bandwidth.

On the other hand, if we integrate the signal at either frequency over the appropriate time inverval by forming $\frac{\int P_{F_1}(t)\,dt}{\int P_{F_2}(t)\,dt}$ we do not obtain information about bandwidth but something is often referred to as "the wavelength dependence of the scatter circuit".

Forming the $\int \frac{P_{F_1}(t)}{P_{F_2}(t)}\,dt$ is one way of obtaining information about bandwidth. Another is the following.

As in the case above we transmit a set of radio waves having different frequency. We now make sure that all these frequencies are correlated in amplitude and phase. This is, as an example, achieved by amplitude modulating a carrier, thus obtaining two sidebands $2f_{AM}$ apart, if f_{AM} is the frequency of the modulating wave. These sidebands, obviously, are correlated in amplitude and phase. At the receiving end we pick up the two sidebands and correlate one with the other (i e we form the cross-correlation function $R_{12}(\gamma)$. The more narrow-banded the transmission channel, the poorer is the correlation. (Transmitting many correlated waves spread over a frequency band, we can find the complete autocorrelation function $R(\Delta F)$ in the frequency domain) as discussed in section 2 above.

This is very analogous, as we shall see in the following, to the power spectrum of the transmission channel.

By analyzing the first alternative first, we can use the results of simple network theory to obtain a simple approximate result. We know that the response to a delta pulse of a network is known as the impulse response $V(\tau)$ of the network. Furthermore, the Fourier transform of the impulse response is known as the transfer function $F(\omega)$ of the network. By multiplying this transfer function with its complex conjugate, we obtain the power spectrum that we are seeking. From the previous section we obtain the expression for the impulse response by taking the square root of equation (3.15). Analyzing this function, we find that it closely resembles an exponential function of the form $P(\tau) = \exp(-\alpha\tau)$. The 1/e width of the impulse response is given by

$$\Delta\tau = d^3 (e^{4/n} - 1)/8aC \qquad (3.17)$$

To simplify the Fourier transformation, we assume an exponential impulse response such that $\Delta\tau = 1/\alpha$ (when we introduce only a small error). The Fourier transform of the exponential impulse response $\exp(-\alpha\tau)$ is given by

$$F(\omega) = (\alpha + j\omega)^{-1}$$

The power spectrum is then given by

$$W(\omega) = F(\omega)\, F^*(\omega)$$

$$= (\alpha^2 + \omega^2)^{-1}$$

Substituting for α as obtained from equation (3.17) and normalizing the resulting equation for $\omega = 0$, we find that the 1/2 power width of the power spectrum is given by

$$\Delta\omega = 8a^2 Cd^{-3} (e^{4/n} - 1)^{-1} \qquad (3.18)$$

Now let us compute the autocorrelation function in the frequency domain $R(\Delta\omega)$. The voltage V_1 at frequency ω is given by $V_1 = F(\omega) = (\alpha + j\omega)^{-1}$. Similarly, the voltage V_2 at frequency $(\omega + \Delta\omega)$ is given by $V_2 = F(\omega+\Delta\omega) = (\alpha+j(\omega+\Delta\omega))^{-1}$. The normalized complex autocorrelation of these two voltages is then given by

$$R(\Delta\omega) = \frac{\int_{-\infty}^{\infty} |1/(\alpha + j\omega)||1/(\alpha - j(\omega + \Delta\omega))|\, d\omega}{\int_{-\infty}^{\infty} |1/(\alpha^2 + \omega^2)|\, d\omega}$$

By solving this integral we get the following expression for the modulus of the autocorrelation function

$$R(\Delta\omega) = |1 + (\Delta\omega/2\alpha)^2|^{-\frac{1}{2}} \qquad (3.19)$$

The width of this autocorrelation function is obtained by letting $R(\Delta\omega) = \frac{1}{2}$, thus obtaining

$$\Delta\omega_{\frac{1}{2}} = 16\sqrt{3}\, a^2 Cd^{-3} (e^{4/n} - 1)^{-1} \qquad (3.20)$$

Note that the width of the autocorrelation in the frequency domain is $2(3)^{\frac{1}{2}}$ times the 1/2-power width of the power spectrum.

3.2.4 Correlation distance of field strength

In this section attention is focused on the spatial field-strength correlation properties of a scattered radio wave. We have a wide-beam transmitter radiating its power essentially in a horizontal direction. The scattered wave resulting from this transmitter impinges on two nearly identical, small-aperture, receiving antennas positioned beyond the horzin relative to the transmitter. The antennas are spaced vertically or

horizontally such that the center line through the receiving antennas is normal to the center line through the transmitter T and the receivers R. We measure the normalized complex correlation of the voltages induced in the antennas.

As shown in section 2 above, this spatial field-strength correlation function is the Fourier transform of the angular power spectrum of the wave reaching the receiving antennas. Specifically, if the antennas are spaced horizontally, thus giving us information about the correlation properties of field strength along a horizontal direction, this correlation function is determined by the angle-of-arrival spectrum as measured in a horizontal plane. If the antennas are spaced vertically, it is the angle-of-arrival spectrum in the vertical plane that matters. Specifying the angle of arrival of a particular scattered wave by an elevation angle α (relative to the center line through T and R) and an azimuth angle β (relative to a great circle plane through T and R), we have in the same manner as above that a refractive-index spectrum $\Phi(K) \sim K^{-n}$ gives rise to an angular power spectrum of the form

$$P(\alpha,\beta) \sim (\beta^2 + \alpha^2)^{-n/2} \qquad (3.21)$$

The horizontal correlation of field strength is thus obtained by a Fourier transformation of P with respect to β, whereas the vertical correlation is obtained from the $P(\alpha)$ relationship.

A rigorous Fourier transformation of expression (2.10), however, lends itself to numerical computations only. In our case, we need a simple approximate expression. This can be obtained if we approximate $P(\alpha)$ and $P(\beta)$ by a $\sin \chi/\chi$ function, thus giving us a simple expression for the Fourier transform. This is a procedure well known in antenna theory. From antenna theory we know that if L is the width of the illuminating field-strength distribution, then the 1/2-power width of the resulting angular power spectrum (beam width) is given by

$$\theta_{\frac{1}{2}} = 0.88\ \lambda/L \qquad (3.22)$$

where λ is the radio wavelength. By applying these results to our problem, we find that the 3-decibel width of the scattered beam as measured in the vertical plane is given by

$$P_{\frac{1}{2}}/P_o = 1/2 = (\alpha_o + \alpha_{\frac{1}{2}}/\alpha_o)^{-n} \qquad (3.23)$$

where $\alpha_{\frac{1}{2}}$ is the 3-decibel beam width of the scattered beam, $\alpha_o = d/2a$, d is the path length, and a is the earth's radius.

By solving for $\alpha_{\frac{1}{2}}$ and substituting this in (3.22), we find that the vertical correlation distance of field strength is given by

$$L_v/\lambda = 0.44\ (\tfrac{a}{d})\ (2^{1/n} - 1) \qquad (3.24)$$

Similarly, the horizontal correlation distance is given by

$$L_H/\lambda = 0.44\ (\tfrac{a}{d})\ (4^{1/n} - 1)^{\frac{1}{2}} \qquad (3.25)$$

These approximate expressions are in very good agreement with the results based on rigorous numerical transformations of the scattered angular power spectra (24).

Note, that the correlation distance is only very weakly related to the spectrum slope and that refraction effects play a dominating role.

3.2.5 Antenna gain degradation

From basic antenna theory we know that the free-space antenna gain is proportional to the antenna aperture $G = 4\pi A\lambda^{-2}$. When dealing with large antennas in connection with scatter

propagation, however, this linear relationship no longer holds. If the antenna aperture is increased by a factor k, the received power is generally increased by a factor that is less than k. This apparent gain degradation is commonly referred to as antenna-to-medium coupling loss. The phenomena can be explained in several different ways. We may base the discussion either on the width of the angular power spectrum of the scattered wave relative to the angular-reception capability of the receiving antenna, or on the spatial correlation distance of the received scattered field strength relative to the dimension of the antenna aperture. In this presentation we shall use the latter method for the purpose of illustrating the principles involved and to get an expression relating the "measured quantity" to the slope n of the refractive-index spectrum, rather than to seek an expression of optimum accuracy.

By basing our computations on the results of the previous section, we note that at the receiving site, the area (normal to the direction of propagation) over which the field strength is correlated is given by $L_v L_H$. This area may then be considered as being the effective receiving antenna aperture, provided that the actual aperture is larger than $L_v L_H$. If the actual area $A < L_v L_H$, we do not experience a gain degradation.

The effective antenna gain is thus

$$G_{eff} = 4\pi L_v L_H \lambda^{-2} \qquad (3.26)$$

whereas the plane-wave gain is

$$G = 4\pi A\lambda^{-2}$$

The gain loss is thus

$$G_L = \frac{A}{L_v L_H} = \frac{5(2^{1/n} - 1)(4^{1/n} - 1)^{\frac{1}{2}} A}{(\frac{a}{d})\lambda^2} \qquad (3.27)$$

Figure 3.9 shows the gain loss plotted against the refractive-index spectrum slope n. It should be emphasized that (3.27) is based on the assumption of isotropy, as are indeed all the expressions for the circuit parameter.

If the atmospheric structure is a horizontally layered one (strongly anisotropic), the spectrum slope n associated with K vertical will be very much different from that associated with K horizontal. Therefore, to calculate the gain loss from (3.27), we shall have to use different values of n for the two directions.

3.2.6 Wavelength dependence of scattered power

Consider now the experiment involving simultaneous transmission and reception on two widely separated frequencies and scaled antennas. If the antenna beams are narrow such that the scattering volume is determined by the beam geometry rather than by the scattering mechanism, then the scattering volumes for the two frequencies are identical. Accordingly, the ratio of the power received on the two frequencies is given by the ratio of the corresponding scattering cross section as presented in (3.13). In this case, therefore, the wavelength dependence is the ratio of power received on the two frequencies given by

$$\left(P(\lambda_1)/P(\lambda_2)\right) = (\lambda_1/\lambda_2)^{n-2} \qquad (3.28)$$

In Figure 3.9 the power ratio is plotted logarithmically to the basis of n and normalized for $n = 6$.

Two different wavelength ratios are used, namely $\lambda_1/\lambda_2 = 3$ and $\lambda_1/\lambda_2 = 5.5$. If for some practical reasons (e g ground reflections) the effective gain of the two scaled antennas are not exactly identical, an error is introduced. It can be shown, however, that the error is proportional to

the square root of the antenna gain ratio only. Note that the term wavelength dependence often refers to the case where the received power is normalized with respect to free-space transmission loss. This normalized power ratio then takes the form

$$\left((P/P_{FS})(\lambda_1)\right)/\left((P/P_{FS})(\lambda_2)\right) = (\lambda_1/\lambda_2)^{n-4} \qquad (3.29)$$

Summing up the section on circuit parameters in relation to scatter propagation in terms of radiometeorological parameters n (refractive index irregularity spectrum) and a (effective earth radius), Table 3.1 and Figure 3.9 are presented.

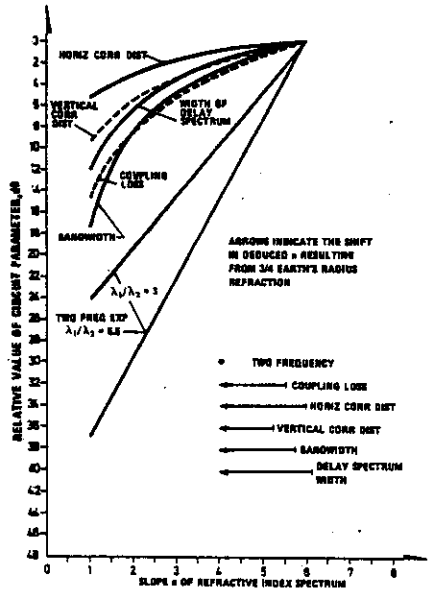

Figure 3.9 The theoretical relationship between the circuit parameter and the slope n of the refractive-index spectrum ($\Phi(K) \sim K^{-n}$). The curves show the degree to which the apectrum slope affects the circuit parameter

COMMUNICATION CIRCUIT PARAMETER	RELATION BETWEEN CIRCUIT PARAMETER AND RADIOMET PARAMETER
WIDTH OF DELAY SPECTRUM	$\Delta\gamma = \frac{d^3}{8a^2c}(e^{2/n}-1)$
BANDWIDTH	$\Delta\omega = \frac{8a^2c}{d^3}(e^{4/n}-1)^{-1}$
GAIN LOSS	$G_L = \frac{5Ad^2}{\lambda a^2}(2^{1/n}-1)(4^{1/n}-1)^{1/2}$
HORIZONTAL FIELDSTRENGTH CORRELATION DISTANCE	$L_H = \frac{0.44\lambda a}{d(4^{1/n}-1)^{1/2}}$
VERTICAL FIELDSTRENGTH CORRELATION DISTANCE	$L_V = \frac{0.44\lambda}{d(2^{1/n}-1)}$
WAVELENGTH	$\frac{P(\lambda_1)}{P(\lambda_2)} = (\frac{\lambda_1}{\lambda_2})^{n-1}$

Table 3.1 Some relationships characterizing a communication channel

3.2.7 Radiometeorological parameters n and a in relation to routine meteorological observations

This topic has been considered in some degree of detail in two earlier publications (25,26). We shall give a summary of the results here. As we have already mentioned, and as will be substantiated in the following section, there are two radiometeorological parameters which are of dominating importance with respect to the characteristic properties of a forward-scatter circuit. One is the effective earth radius a , the other is the spectrum slope n of the refractive index irregularity spectrum. We shall now discuss the relationship between purely meteorological factors and the parameters a and n.

A Determination of effective earth radius a from radiosonde measurements

The refractivity N (where $N = (n - 1)\ 10^6$, n being the refractive index) is obtained from meteorological parameters by the Debye relationship

$$N = 77 \cdot 6 \frac{P}{T} + 3.73 \times 10^5 \frac{e}{T^2} \qquad (3.30)$$

where P is the total pressure in millibars, T the absolute temperature, and e the water vapour pressure in millibars. Thus from knowledge about the vertical profile of P, T, and e as obtained from a conventional radiosonde, we can calculate the refractivity profile.

Knowing the N profile, we can calculate the ray bending from Snell's law (see section 3.1 above). We are thus able to calculate the total bending to which a ray is subjected, when propagating from the transmitter to the centre of the scattering volume.

Similarly, we can calculate the bending experienced from the midpath point to the receiver. (In practice, we perform the calculation from the receiver back to the mid-path point). We then know the effective scattering angle, which is the difference between the angle between the earth tangent planes through the transmitter and receiver and the total ray bending.

If d is the distance between the transmitter and receiver, then the angle θ between the tangent planes is given by

$$\theta = \frac{d}{R}$$

where R is the real earth radius. By the same relationship, we then obtain the effective earth radius a using the effective scattering angle.

Alternatively, if the refractivity gradient dN/dz is constant through the height interval involved (from ground to scattering volume), then the effective earth radius is given by the simple relationship

$$\frac{1}{a} = \frac{1}{R} + \frac{dN}{dz} \times 10^{-6}$$

assuming a near-horizontal direction of the radio beam.

We observe, then, that on the basis of P, T, and e, data from a conventional radiosonde ascent, we can obtain the radio-meteorological parameter a appropriate for a given height of the scattering volume (corresponding to a given path length). The solid lines in Figure 3.10 show probability distribution of the ratio a/R based on 230 radio soundings at Sola in South-Western Norway during 1966 (14).

For comparison, the dashed line shows the ratio a/R based on 45 radiosonde ascents during October and November 1970 at Maniwaki, near Ottawa, Canada. This line lies intermediate to the Sola curves, but has a slope similar to the Norwegian summer data.

B Determination of spectrum slope n from radiosonde measurements

Here the reader is referred to (25), where an empirical relationship was found between the atmospheric stability (a somewhat modified version of the well-known Väisälä-Brunt frequency v^2) and the slope n of the refractive inded irregularity spectrum. The conventional Väisälä-Brunt frequency appears as the numerator in the Richardson's number and is normally written as

$$v^2 = \frac{g}{T}\left(\frac{dT}{dz} + \frac{g}{c_p}\right) \qquad (3.31)$$

Here g is the gravitational constant, T the temperature, dT/dz the vertical temperature lapse rate, and c_p the specific heat at constant pressure. We see that the expression whitin the brackets is a measure of the difference between the actual temperature lapse rate and the adiabatic lapse rate. This expression normally refers to a limited vertical section of the atmosphere.

The correlation of the spectrum slope n with atmospheric parameters describing the dynamic state of the atmosphere was significantly improved when a particular weighting function was placed on the temperature contribution to the stability.

Specifically, by adding a number which is determined by the temperature at the 850 mbar surface (1500 m altitude) to the Väisälä-Brunt frequency, the $n - v^2$ correlation was improved. For our particular purpose therefore, a modified version of v^2 was used:

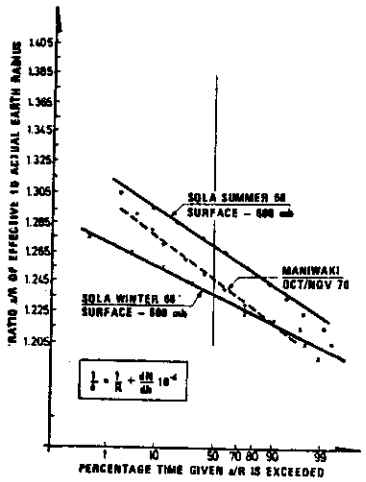

Figure 3.10 Distributions of the ratio of effective to actual earth radius, based on radiosonde observations at Sola, Norway and Maniwaki, Canada

$$v^2 = \frac{g}{T}\left(\frac{dT}{dz} + 5.50 \times 10^{-3}\, T_{850} + \frac{g}{c_p}\right) \qquad (3.32)$$

Here T, measured in degrees K, and dT/dz, in degrees per 100 m, are average values obtained over the 850 - 400 mbar levels (1.5 to 7 km altitude).

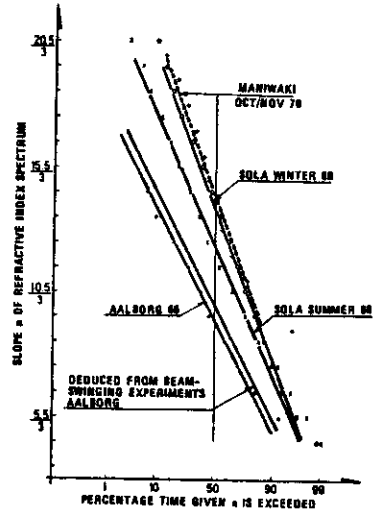

Figure 3.11 Distributions of the slope of the spectrum of refractive index irregularities as deduced from radiosonde observations and beam-swinging experiments

Having obtained v^2 from the results of a temperature profile determined by a conventional radiosonde observation, the spectrum slope n is found, using the expression for the n versus v^2 regression line:

$$n = 40.6 + 708\, v^2 \qquad (3.33)$$

Figure 3.11 shows probability distributions of spectrum slope n. The two upper curves are for the radiosonde station Sola in South-Western Norway for summer and winter 1966. These curves correspond to the distributions of Figure 3.10 and form the basis for the calculations to be presented in the following

sections. For comparison, Figure 3.11 also shows n distributions for Mainwaki and for Aalborg, Northern Denmark, as obtained on the basis of radiosondes. The "predicted" n distribution for Aalborg is compared with that deduced from radio beam-swing experiments (10,16).

C Channel characterization statistics on the basis of meteorological data

From the chapter above, we are in a position to calculate the probability distributions for some of the important transmission channel parameters.

From the meteorological data as converted to the radiometeorological parameters n and a and presented in Figures 3.10 and 3.11, we are able to calculate channel parameters such as pulse distortion and bandwidth from the list of basic expressions given in Table 3.1.

A set of such probability distributions is given in Figures 3.12 to 3.17 (for further details on other channel characterization parameters, the reader is referred to ref (26)).

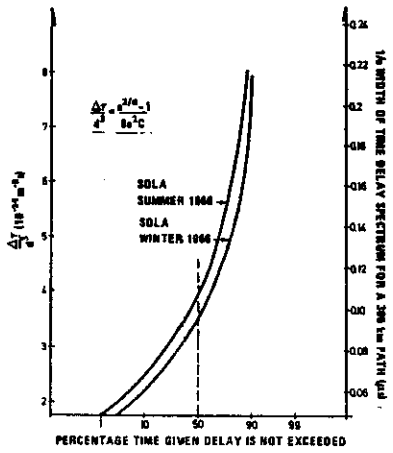

Figure 3.12

Width $\Delta\tau$ of the time delay function

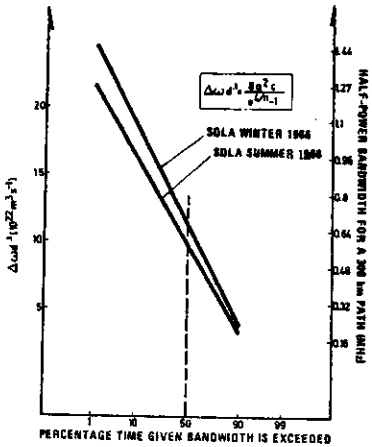

Figure 3.13

Half-power bandwidth $\Delta\omega$

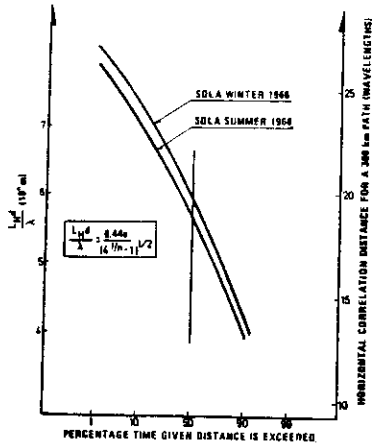

Figure 3.14

Horizontal field strength correlation distance

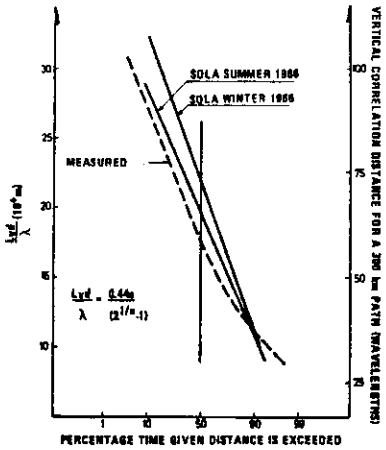

Figure 3.15

Vertical field strength correlation distance (24)

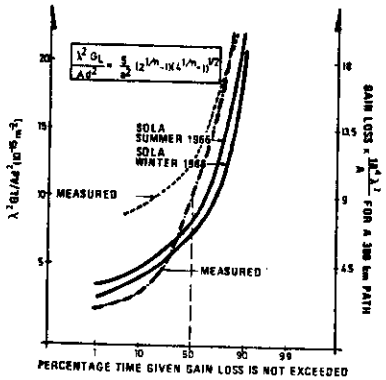

Figure 3.16

Antenna gain loss G_L (24,27)

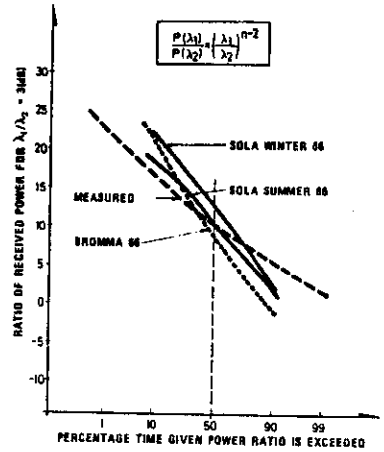

Figure 3.17

Ratio of received power for a wavelength ratio of 3 (18)

3.2.8 Scattering from atmospheric layers (waves)

In the previous chapter, the theory was based on the assumption that the refractive index irregularities were distributed randomly in the atmosphere, and superimposed on a gradual decrease of refractive index with height. We shall now consider another extreme case where the scattering/reflection largely is a result of a thin strata through which the refractive index varies drastically. For the purpose of illustrating the physics and the fundamental principles of the problem at hand, we shall explicitly present three different idealized atmospheric structures. These are shown in figure 3.18. Here the first sketch (a) refers to the case we have discussed in the previous section. Sketch (b) will now be considered. Here we assume an irregular refractive index profile characterized by a layer of thickness Δh, through which refractive index varies linearly by total amount Δn.

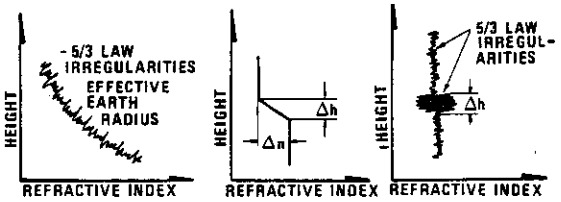

Figure 3.18 The categories of atmospheric structure under consideration

As we have already inferred above, and treated in detail in section 2.2, the angular power spectrum of the scattered (reflected) wave is obtained by a simple Fourier transformation of the refractive index profile within the scattering volume. This procedure has been substantiated by several authors i e J Wait, see ref (28).

$$|\sigma|^2 = \left| \frac{\Delta n}{2 \sin^2 (\frac{\theta}{2})} \left(\frac{\sin X}{X}\right) \right|^2 \qquad (3.34)$$

Here X is a function of the geometry as follows

$$X = \frac{2\pi \Delta h}{\lambda} \sin \theta/2$$

where θ is the scattering angle.

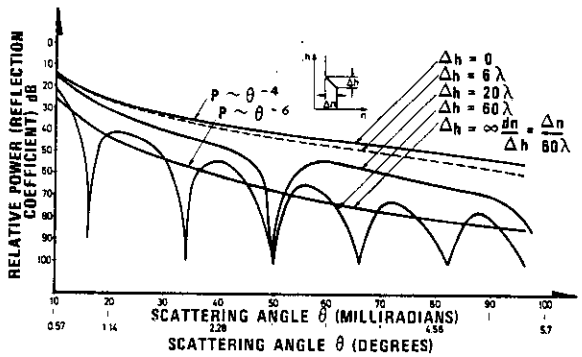

Figure 3.19 Angular power spectrum of a scattered wave resulting from a layer of thickness Δh

This function is plotted to the basis of scattering angle for various layer thicknesses in figure 3.19.

The two limiting cases are an infinitesimally thin layer ($\Delta h = 0$) and an infinitely thick layer ($\Delta h = \infty$). For $\Delta h = 0$ it can readily be verified that the power reflection coefficient is given by

$$|\sigma|^2 = \left| \frac{\Delta n}{2 \sin^2 \theta/2} \right|^2 \qquad (3.35)$$

$$\text{i e} \quad P(\theta) \sim \theta^{-4} \qquad (3.36$$

We see that an infinitesimally thin layer (discontinuity in n) gives rise to a scattering-angle dependence of scattered power which is very close to the $-\frac{11}{3}$ law obtained for homogeneous isotropic inertial subrange turbulence. A layer of finite thickness results in an oscillatory dependence of the reflection coefficient on the scattering angle. The thicker the layer is, the more rapid are the oscillations. When the layer thickness approaches infinity, i e, when we remove the upper knee of the profile, the oscillator angular dependence disappears since we no longer get interference between the two boundaries. The result is a smooth angular spectrum given by

$$|\sigma|^2 = \left(\frac{dn}{dh} \frac{\lambda}{8\pi \sin^3 \theta/2}\right)^2 \qquad (3.37)$$

$$\text{i e} \quad P(\theta) \sim \theta^{-6}$$

We may conclude, therefore, that a single atmospheric layer gives rise to angular dependences varying from $\theta^{-4} - \theta^{-6}$ depending on the layer thickness. The power scattered in a given direction is determined by layer thickness and by the change in refractive index through the layer.

However, no single layer can give an angular dependence weaker than that corresponding to the θ^{-4} law.

Finally we shall consider the spatially intermittent type structure shown in figure 3.18c. We shall see to what extent such a structure influences the angular power spectrum.

In order to simplify the treatment, we shall assume that the variance of the refractivity irregularities through the turbulent stratum is given by a $(\sin x)/x$ relationship and that the spectrum of the irregularities can be written in the form K^{-n}.

The resultant spectrum is a convolution integral where the K^{-n} spectrum is convolved with the spectrum of the $(\sin x)/x$ filter function. The spectrum of the $(\sin x)/x$ filter is a rectangular function. The width of this rectangular filter spectrum is taken to be $2K'$ and the density A is taken as $\frac{1}{2} K'$ such that the integral of the filter spectrum becomes unity. The power spectrum of such a turbulent stratum then becomes

$$E(K) = \int_{K-K'}^{K+K'} ACK^{-n} \, dK$$

Solving this simple integral we get

$$E(K) = AC\left(2K'K^{-n} + \frac{2}{3!}(1-n)(-n-1)\, K'^3 K^{-n-2} + \frac{2}{5!}\left((1-n)(-n-1)(-n-2)(-n-3)\, K'^5 K^{-n-4}\right)\right)$$

Choosing then $n = 4 = \frac{11}{3}$ we get

$$E(K) = K^{-4}\left(1 + 10/3\left(\frac{K}{K'}\right)^{-2} + 7\left(\frac{K}{K'}\right)^{-4} + \ldots\right) \qquad (3.38)$$

Figure 3.20 shows a graphical representation of this equation. We see that unless the thickness of the stratum is less than 2 or 3 times the projected wavelength $\lambda/\sin\theta/2$, the spatial intermittency of the refractive index irregularities has no influence on the angular spectrum of the scattered wave.

Furthermore, we know that all irregularities within the scattering volume contribute to the scattered field strength at the receiver. A very thin turbulent layer must therefore have a very large variance in order to give a contribution which is comparable with that of the background turbulence in which the stratum is assumed to be embedded (29).

Finally, we see from figure 3.20 that the existence of turbulent layer results in a spectrum slope which is steeper than that one would have with $-\frac{5}{3}$ law homogeneous turbulence.

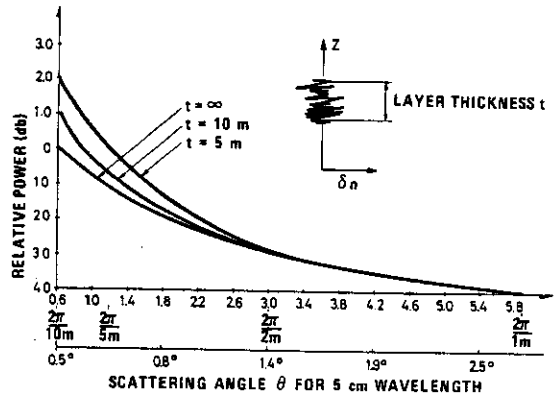

Figure 3.20 Angular power spectrum of a scattered wave resulting from a thin stratum of intense turbulence

Transmission loss as a function of carrier frequency

Consider now the experiment involving simultaneous transmission and reception on two widely separated frequencies and scaled antennas. If the antenna beams are narrow such that the scattering volume is determined by beam geometry and not by the scattering mechanism, then the scattering volumes for the two frequencies are identical. Measuring then the ratio of the power received on the two frequencies, we get information about the refractive index spectrum along a vertical direction within the scattering volume. Writing this spectrum as $\Phi(K) \sim K^{-n}$, the power ratio is simply given by

$$\frac{P(\lambda_1)}{P(\lambda_2)} = \left(\frac{\lambda_1}{\lambda_2}\right)^{n-2} \tag{3.39}$$

If the received power is normalized with respect to the free-space transmission loss, the corresponding power ratio becomes

$$\frac{\frac{P}{P_{FS}}(\lambda_1)}{\frac{P}{P_{FS}}(\lambda_2)} = \left(\frac{\lambda_1}{\lambda_2}\right)^{n-4} \tag{3.40}$$

We see that atmospheric refraction does not enter the equation in this case.

Spatial correlation properties of field strength

We have a wide-beam transmitter radiating its power essentially in a horizontal direction. The resulting scattered wave is received by two nearly identical, small aperture, receiving antennas positioned beyond the horizon relative to the transmitter.

The antennas are spaced vertically or horizontally such that the centre line through the receiving antennas is normal to the

line through the transmitter and the receivers. We measure the normalized complex correlation of the voltages induced in the antennas.

As we have already seen (section 2.2), this spatial field-strength correlation function is the Fourier transform of the angular power spectrum of the wave reaching the receiving antennas. Thus if the antennas are spaced vertically, the correlation distance of field-strength gives us information about the angle-of-arrival spectrum in the vertical plane. Similarly, horizontally spaced antennas give us information about the angular spectrum in a horizontal plane.

Referring to section 3.2.4 above, the vertical correlation distance is given by

$$\frac{L_V}{\lambda} = 0.44 \frac{a}{d} (2^{1/n} - 1)^{-1} \qquad (3.41)$$

and the horizontal correlation distance

$$\frac{L_H}{\lambda} = 0.44 \frac{a}{d} (4^{1/n} - 1)^{-\frac{1}{2}} \qquad (3.42)$$

where a is the effective Earth radius (i e refraction effects are important), d the path length and n the slope of the irregularity spectrum within the scattering volume ($\Phi(K) \sim K^{-n}$). The vertical correlation distance is determined by the vertical component of the three-dimensional spectrum whereas the horizontal correlation distance is governed by the spectrum along a direction which is determined by the length of the path. For a line of sight path (if a scatter experiment could be realized on such a path), it is the horizontal component of the three-dimensional spectrum that matters. If the path length is large, it is the component along a direction which is close to being vertical that has the dominating influence (25).

Antenna gain degradation

As we have already seen (section 3.2.5 above), the gain loss is inversely proportional to the product of the vertical and horizontal correlation distances. Thus inespective of whether we are dealing with homogeneous a random turbulent atmosphere as one which is characterized by a layered structure, the gain loss is given by:

$$G_L = \frac{A}{L_V L_H} = \frac{5(2^{1/n} - 1)(4^{1/n} - 1)^{\frac{1}{2}} A}{(a/d)^2 \lambda^2} \qquad (3.43)$$

Note that this equation is based on the assumption that the transmitting antenna beam is broad both in azimuth and elevation and the receiving eam narrow in both planes. This condition is necessary for the influence of the atmospheric structure on the gain loss to be a maximum.

Time delay

The mechanisms we have discussed so far, all rely directly or indirectly on the angular power spectrum of the scattered wave. We have seen that the two extreme structure categories, homogeneous $-\frac{11}{3}$ law turbulence and single, infinitesimally thin layer, give angular spectra which for all practical purposes are indistinguishable.

Admittedly there are special sets of e g, beamswinging experiments, that at least in principle can reveal the differences but on the basis of simple single experiments and reasonable beamwidths, it is very difficult to analyse a single-layer structure.

The two remaining circuit parameters to be discussed, time delay and bandwidth measurements, do not rely on the angular power spectrum but on the delay function. Using wide-beam antennas on either end such that the multipath transmission is

governed by the scattering mechanism rather than by beam geometry, we seek an expression relating path length ℓ and the position in space of the scattering element (layer). Note that the loci of constant delay in a forward scatter circuit are concentric ellipsoidal surfaces having the transmitting and receiving points as foci. Discussing then layers which are predominantly horizontal, we see that those in the neighbourhood of the mid-path point of interest in a forward-scatter experiment coincide with the constant-delay surface. It is thus essentially the vertical distribution of scatterers which matters in a pulse-delay experiment.

Simple geometry shows that if θ is the scattering angle corresponding to a given path length ℓ, and d the length of the chord between the transmitter and the receiver, then ℓ and θ are related by the following equation

$$\theta = 2\left(\left(\frac{\ell}{d}\right)^2 - 1\right)^{\frac{1}{2}} \tag{3.44}$$

Differentiating this equation so as to get an expression for $d\ell/d\theta$, we find the following relationship between $\Delta\theta$ and $\Delta\ell$:

$$\Delta\theta = \frac{4\ell}{d^2\theta}\,\Delta\ell \tag{3.45}$$

Neglecting second-order terms and putting $\Delta\theta = \Delta z/(d/2)$ and $\theta = d/a$, where Δz is the height coordinate measured from the intersecting point of the two tangent planes through T and R, and a, as usual, is the effective Earth radius, we get the following expression

$$\Delta\ell \approx \frac{2d}{a}\,\Delta z \tag{3.46}$$

If then the refractive index irregularities are limited to a layer or thin strata of thickness Δz, then a delta pulse transmitted at T will appear as a broadened pulse, or a

spectrum of delta pulses at R, and the width of this delay spectrum is given by

$$\Delta\gamma = \frac{\Delta\ell}{c} = \frac{2d}{ac}\,\Delta z \tag{3.47}$$

where c is the wave velocity.

As an example, consider a 200-km path and a thickness of the turbulent strata of 10 m. From Equation (3.46) we then see that path length difference $\Delta\ell$ will be

$$\Delta\ell = \frac{1}{15}\,\Delta z$$

The width of the delay spectrum $\Delta\gamma$ associated with a 10-m thick stratum will then be

$$\Delta\gamma \approx 2 \times 10^{-3}\ \mu s$$

Assume now, that the thin layer is embedded in a background of turbulence and that his turbulence gives rise to a $-\frac{11}{3}$ law refractive index irregularity spectrum. We have previously shown that the 1/e width of the delay spectrum resulting from a homogeneous irregularity spectrum is given by

$$\Delta\gamma = \frac{d^3}{8a^2c}\left(e^{2/n} - 1\right) \tag{3.48}$$

where n is the slope of the irregularity spectrum. This should be $\frac{11}{3}$ for homogeneous isotropic inertial subrange turbulence. Using the same path geometry as in the above example, we find from Equation (3.48) that the width of the delay spectrum resulting from the background turbulence is

$$\Delta\gamma = 60 \times 10^{-3} \ \mu s$$

This is a factor 30 relative to the delay spectrum width resulting from a 10-m thick layer. The background turbulence, however, will give a particular decrease in intensity with increasing delay whereas a thin layer of large refractive index variance will give a well defined peak in the delay spectrum.

Bandwidth

Our interest is now finally focused on the bandwidth properties of a scattered wave in relation to the particular atmospheric structures under consideration.

We have previously shown (section 2.1 above) that there is a simple relationship between the width of the delay spectrum and the bandwidth. If $\Delta\gamma$ is the width of the rectangular delay spectrum resulting from a layer of thickness Δz, then the bandwidth Δf is given by

$$\Delta f = \frac{1}{\Delta\gamma} = \frac{c}{\Delta\ell}$$

From Equation (5.47) above then, we get

$$\Delta f = \frac{ac}{2d\Delta z}$$

On the basis of the previous example with a 10-m thick layer within the scattering volume limited by broad beams and a 200-km path, we find that the bandwidth

$$\Delta f = 500 \text{ MHz}$$

Then let us consider the bandwidth limitation resulting from the background turbulence. We have already shown that this bandwidth is given by

$$\Delta f = \frac{8a^2c}{2\pi d^3 (e^{4/n} - 1)} \tag{3.49}$$

For $n = \frac{11}{3}$ (inertial subrange turbulence) we find that the bandwidth corresponding to a 200-km path is

$$\Delta f = 1.2 \text{ MHz}$$

We see that the contribution to the bandwidth of the background turbulence is very small compared with that of a thin layer (30 - 38).

Table 3.2 summarizes the theoretically obtained relationships pertaining to forward scattering from turbulence and from stratified layers.

Propagation parameter \ Atmospheric structure	Background turbulence	Thin layer
Angular powerspectrum	$\frac{P(\theta)}{P(\theta_0)} = (1 + \frac{\theta}{d/a})^{-(11/3+1)}$	$\frac{P(\theta)}{P(\theta_0)} = (1 + \frac{\theta}{d/a})^{-4}$
Wavelength dependance	$\frac{P(\lambda_1)}{P(\lambda_2)} = (\frac{\lambda_1}{\lambda_2})^{11/3-2}$	$\frac{P(\lambda_1)}{P(\lambda_2)} = (\frac{\lambda_1}{\lambda_2})^{4-2}$
Vertical E-correlation	$\frac{L_V}{\lambda} = \frac{0.44\ a}{d(2^{3/11} - 1)}$	$\frac{L_V}{\lambda} = \frac{0.44\ a}{d(2^{1/4} - 1)}$
Horizontal E-correlation	$\frac{L_H}{\lambda} = \frac{0.44\ a}{d(4^{3/11} - 1)^{\frac{1}{2}}}$	$\frac{L_V}{\lambda} = \frac{0.44\ a}{d(4^{1/4} - 1)^{\frac{1}{2}}}$
Coupling loss	$G_L = \frac{5A(2^{3/11} - 1)(4^{3/11} - 1)^{\frac{1}{2}}}{(a/d)^2 \lambda^2}$	$G_L = \frac{5A(2^{1/4} - 1)(4^{1/4} - 1)^{\frac{1}{2}}}{(a/d)^2 \lambda^2}$
Pulse delay	$\Delta\tau = \frac{d^3}{8a^2c}(e^{8/11} - 1)$ 200-km path $\Delta\tau = 60$ ns	$\Delta\tau = \frac{2d}{ac}\Delta h$ 200-km path, h = 10 m $\Delta\tau = 2$ ns
Bandwidth	$\Delta f = \frac{8a^2c}{2\pi d^3 (e^{12/11} - 1)}$ 200-km path $\Delta f = 1.2$ MHz	$\Delta f = \frac{ac}{2d\Delta h}$ 200-km path, h = 10 m $\Delta f = 500$ MHz

Table 3.2 Some theoretical relationships pertaining to forward scattering from turbulence and stratified layers

In summing up this section on propagation mechanisms involving scattering and reflection, the following should be noted: The parameters characterizing the transmission medium exhibits dramatic variations with time. When illuminating a target through this variable propagation medium, one should bear in mind that the propagation conditions can be favourable during small time intervals only. To achieve maximum radar target resolution, therefore, we shall have to take many "snapshots" and select the data sets which gives optimum resolution (contrast).

3.2.9 Scattering by particles (rainfall)

A review on propagation mechanisms in relation to adaptive radar systems would be imcomplete if the phenomena related to rainfall were not discussed.

In this presentation a simple qualitative discussion will be given. For details, the reader is referred to e g (2, 38, 39, 40).

When studying the effect of precipitation on electromagnetic waves, several fa tors describing the rain structure should be considered. These are:

- Rainfall rate
- Drop-size distribution
- Shape of raindrops
- Canting angle of raindrops (orientation in space of ellipsoidal raindrops)

Rainfall rate and drop size distribution are, evidently, the most important parameters.

Consider a dielectric sphere of diameter D in an electromagnetic field where the wavelength λ is large compared with the

diameter of the sphere. The sphere will give rise to an induced dipole moment as discussed in chapter 2 above, and reradiate the power which has been extracted from the incident electromagnetic field in all directions.

The region where the diameter of the sphere is very long compared with the wavelength is known as the Rayleigh region. The analysis related to this case is well known and leads to the result that the scattering cross-section of the sphere increases as the fourth power of frequency. If the sphere has a complex dielectric constant, part of the power incident on the sphere is dissipated as heat and consequently causes a reduction in the amount of reradiated power.

Increasing now the frequency of incident radiation such that its wavelength becomes comparable with the dimensions of the dielectric sphere, the problem rapidly becomes complex. One now will have to consider the field patterns within the sphere. The simplest pattern is that obtained when the circumference of the sphere is one wavelength. We then have a condition which is referred to as dipole resonance giving maximum scattering cross-section. Increasing the frequency further, a situation characterized by quadrupole resonance occurs when the circumference is two wavelengths long. Decreasing the wavelength of the field still further, hexapole resonance conditions are reached, followed by octopole, and so on until the cross-section becomes a highly complex linear superposition of these multipole radiators which finally converge to the limit known as the "geometrical" value.

Normalizing the scattering cross-section to this value, the scattering cross-section versus frequency dependence is shown in figure 3.21.

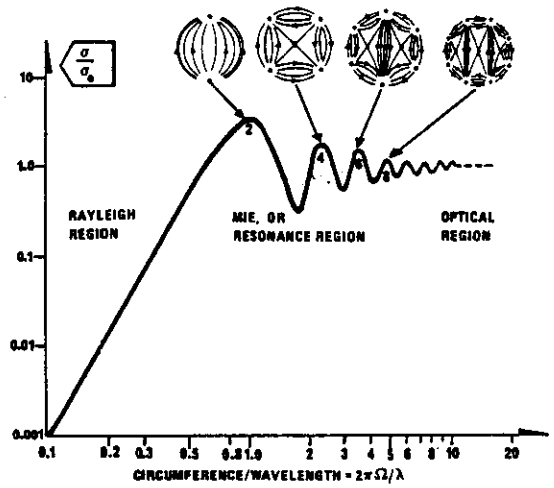

Figure 3.21 Normalized scattering cross-section of a dielectric sphere as a function of normalized wavelength

3.3 Diffraction of radio waves by obstacles

Radio propagation over natural obstructions has been a subject of considerable interest. Classical knife-edge diffraction theory is used as an idealization of the physical problem. However, due to difficulties in obtaining an analytical solution, particularly when ground reflections and complex obstacles are considered, most of the previous work has been restricted to compilations of results from theory and measurements, i e magnitude considerations only.

The knife-edge diffraction problem has been formally solved by several techniques. The early work by Sommerfeld, who based his analysis on the wave equation with appropriate boundary conditions, is perfectly rigorous and not restricted to small diffracting angles, but generalization to the multiple-reflection problem is not readily accomplished.

Fresnel and Kirchhoff based their work on an analytic formulation of Huygen's principle. The Fresnel-Kirchhoff method has the advantage of the simplicity of ray-path concept, and is used almost exclusively in radio propagation literature. However, the method suffers from lack of rigor and from the appearance of the Fresnel integrals which tend to obscure physical interpretations. In order to obtain practical solutions to the problem of diffraction in the presence of multiple reflections, a phasor summation of the Fresnel-Kirchhoff results is performed for the single ray problem.

In a paper by Ratcliffe (42) a very neat and general method for solving complex diffraction problems is sketched. Ratcliffe shows that if, in particular, a one-dimensional diffracting screen is illuminated by a wave (wavelength λ), then the angular power-spectrum $P(\theta)$ produced, expressed in terms of $\sin\theta$, is the Fourier transform of the spatial distribution $E(z)$ of the wave front just as it leaves the screen, provided z is expressed in terms of λ.

Basic theory of diffraction

Our problem is the following:

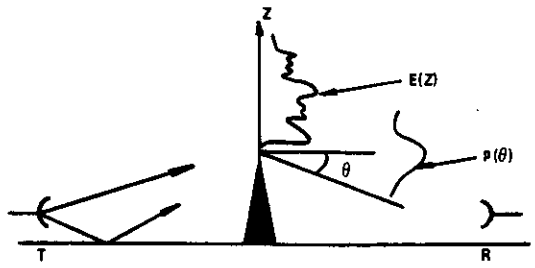

Figure 3.22 Geometry of the diffraction problem

The transmitter illuminates a region above the obstacle. This gives rise to a distribution of field strength along a vertical direction above the obstacle. This distribution is determined by multipath effects, by the ground reflection coefficient, and by the radiation properties of the antenna. On the basis of knowledge about $E(z)$, we want to calculate the angular power spectrum $P(\theta)$ of the diffracted wave.

We now use exactly the same approach as for the scatter propagation (case discussed in chapter 2) and derive the following expression for the secondary field E_s, (scattered field or diffracted field as the case may be):

$$E_s(K) = \frac{k^2}{4\pi R} \int E_o(z)\ \varepsilon(z)\ e^{-jKz}\ dz \qquad (3.50)$$

where

R = distance between receiver and diffraction element (distance from obstacle)

$|k| = \frac{2\pi}{\lambda}$ where λ is the wavelength

$\vec{K} = \vec{k}_{in} - \vec{k}_{sc}$ and $|\vec{K}| = \frac{4\pi}{\lambda} \sin \theta/2$

$\varepsilon(z)$ = distribution of permittivity above the obstacle

$E_o(z)$ = distribution of field strength above the obstacle

θ = essentially the direction of the diffracted wave under consideration.

Thus the angular distribution ($\vec{K}$ distribution) of the secondary field is the Fourier transform of the $E_o(z)\ \varepsilon(z)$ product.

Two limiting cases are of interest:

a) If the field E_o incident on the plane above the obstacle varies far more rapidly with height z than does $\varepsilon(z)$, then $\varepsilon(z)$ does not contribute to the convolution and we can put $\varepsilon(z)$ outside the Fourier integral. We th s have an important relation: *The angular distribution of the diffracted wave is the Fourier transform of the field strength distribution measured in a plane above the obstacle giving rise to diffraction.*

b) Conversely, if $\varepsilon(z)$ varies rapidly in relation to $E_o(z)$, then $E_o(z)$ does not contribute to the convolution and we have an expression for the scattered wave. *The angular distribution of the scattered waves is the Fourier transform of the permittivity (refractive index) distribution.*

Thus, if we want to calculate the transmission loss resulting from a given obstacle, the procedure is in short the following:

Step 1

Calculate the field strength distribution along a vertical direction over the obstacle, considering the influence of ground reflections, etc. Note that if the obstacle cannot be considered as a knife edge, then reflection from the obstacle itself may contribute to the field strength distribution over the ridge.

Step 2

Having obtained an expression for $E_o(z)$, we compute the Fourier transform of $E_o(z)$, thus obtaining the angular field strength distribution $E_s(\theta)$ of the diffracted wave. In order to obtain the angular power distribution $P(\theta)$, we shall have to multiply $E_s(\theta)$ with its complex conjugate $E_s^*(\theta)$.

Note that in order for this Fourier transformation to be dimensionally meaningful, the space coordinate will have to be normalized with respect to wavelength. The direction θ is then to be expressed in terms of sin θ.

Step 3

Having obtained the angular power spectrum $P(\theta)$, we shall essentially have to repeat step number one in order to obtain the desired expression for the power received at a given point in the diffraction zone behind the obstacle.

We shall now consider this procedure in some degree of detail.

Let us then first calculate the field strength distribution above the obstacle.

In order to obtain simple, comparatively general and in particular physically interpretable expressions for the field strength distribution above the obstacle (first step in the procedure) we shall have to idealize the problem and in doing so make certain approximations. Let us consider the case with one direct and one reflected wave.

We then see that the most striking feature of the vertical field strength distribution is the periodicity. We clearly have a component of field strength which varies in a sinusoidal fashion with height.

From knowledge about the reflection properties of surfaces under various degrees of roughness, one would expect the influence of multipath on the vertical field strength profile to diminish with height. Hence one would expect the sinusoidal field strength oscillation to be damped in some manner. Lastly, we see that the DC level of the $E_o(z)$ profile is a parameter of some importance.

Our diffraction problem will therefore be based on the following field strength profile:

- a constant term E_1
- a damped sinusoidal term given by $E_2(z) = E_2 e^{-\alpha z k} \sin \frac{2\pi}{L} z$

Note that the vertical coordinate z is measured in terms of number of wavelengths.

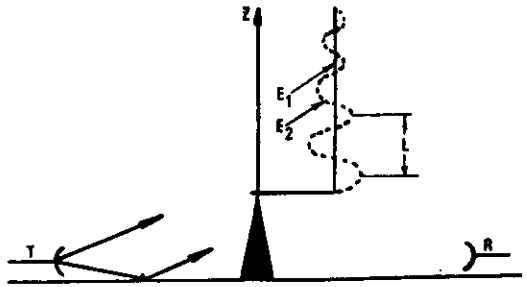

Figure 3.23 Vertical fieldstrength distribution with ground reflections

Angular spectrum of diffracted field

The nect step in the calculation involves a Fourier transformation of the vertical field strength profile.

a) The first term in the expression for the field is a step function

$$E_1(z) = \begin{cases} 0 & \text{for } z < 0 \\ 1 & \text{for } z > 0 \end{cases}$$

The Fourier transform of this is the following

$$F_1(\theta) = \tfrac{1}{2}\delta(\theta) + \frac{1}{j\theta} \qquad (3.51)$$

This assumes small angles θ such that $\theta \approx \sin\theta$. Note that δ is a Dirac delta function.

b) For simplicity we write the second term as follows

$$E_2(z) = E_2\, e^{-\alpha kz} \sin \beta kz \qquad (3.52)$$

such that $\beta = \lambda/L$.

This function gives a comparatively simple Fourier transform, namely

$$F_2(\theta) = \frac{\beta}{\alpha^2 + \beta^2 - \theta^2 + 2j\alpha\theta} \qquad (3.53)$$

such that the resultant angular spectrum is given by

$$F(\theta) = F_2(\theta) + F_1(\theta)$$

$$= \frac{\beta E_2}{\alpha^2 + \beta^2 - \theta^2 + 2j\alpha\theta} + \frac{E_1}{j\theta} \qquad (3.54)$$

The angular power spectrum is then obtained from the following

$$P(\theta) = F(\theta) \cdot F^*(\theta)$$

This function has a pronounced maximum for a certain direction, namely the direction corresponding to

$$\theta = \pm \sqrt{\beta^2 + \alpha^2}$$

If we have no damping, i e if $\alpha = 0$, then we have a Dirac delta function for $F_2(\theta)$ centered at

$$\theta = \beta \quad \text{i e at} \quad \theta = \frac{\lambda}{L}$$

This is the same as the results obtained using the Bragg scattering relationship in connection with the scattering from sinusoidal variations with height of the refractive index. From Bragg we have the following.

Maximum scatter in a direction θ given by

$$K = \frac{4\pi}{\lambda} \sin \theta/2$$

where $K = 2\pi/L$. As in the diffraction case above, L is the period in space of the sinusoidal variations, i e

$$\frac{2\pi}{L} = \frac{4\pi}{\lambda} \theta/2$$

i e $\theta = \lambda/L$

as we obtained above.

We know that a single ground reflected component interfering with the direct wave will give a field strength distribution

above the obstacle of the form given in equation (3.54) above. The damping factor α will then be determined by the rate at which the ground reflection coefficient decreases with increasing angle of incidence to the ground. The period of oscillation, L, is given by the geometry. Let R be the distance between transmitter and knife-edge obstacle, h the height of the transmitter above the flat earth and λ the radio wavelength; then the period L is given by

$$L = \frac{\lambda R}{2h} \tag{3.55}$$

Thus, in this case, we will have maximum energy diffracted in a direction given by

$$\theta = \frac{2h}{R} \tag{3.56}$$

Thus, by adjusting the height, h, of the transmitting antenna, we can beam the diffracted wave in the desired direction. We see that ground reflection (leading to an oscillating vertical profile of field strength) actually increases the power received at a given point behind the obstacle. This increase is known as <u>obstacle gain</u>. Note that we shall have to transform the coordinate system such that θ is measured relative to the line joining the top of the knife-edge obstacle and the transmitter and not relative to the horizontal line through the obstacle top.

Let us now, as an example, calculate the obstacle gain. As we have seen, the diffracted field, F_1, resulting from the unit step function (the DC term) is given by

$$F_1 = \frac{E_1}{j\theta}$$

The maximum field resulting from the oscillating term (i e field in direction θ where $\theta = \sqrt{\alpha^2 + \beta^2}$) is, as seen from equation (3.54), given by

$$F_2 = \frac{E_2 \beta}{j2\alpha \sqrt{\alpha^2 + \beta^2}} \tag{3.57}$$

"Obstacle gain" or "multipath gain" is then

$$G_o = \left(\frac{F_2 + F_1}{F_1}\right)^2 = \left(\left(\frac{E_2}{E_1}\right)\left(\frac{\beta}{2\alpha}\right) + 1\right)^2 \tag{3.58}$$

Note that this gain refers to the direction $\theta = \sqrt{\alpha^2 + \beta^2} = \sqrt{\left(\frac{\lambda}{L}\right)^2 + \alpha^2}$

where L is the spatial period of field strength oscillations.

We see from this equation that the diffraction loss relative to that of the no-multipath case can be reduced considerably by a proper adapting of the appropriate parameters, i e

- making the field strength oscillations above the obstacle as deep as possible by making the direct wave comparable in magnitude with that of the interfering wave (in equation (3.54) $E_2 \rightarrow E_1$)

- reducing the damping factor, α, by seeking ground reflections from a surface giving a small decrease in reflection coefficient with angle of incidence.

Tables 3.3 og 3.4 give some practical examples.

α/β	0.2					
E_2/E_1	1	0.8	0.6	0.4	0.2	0
Obstacle gain G_o dB	10.8	9.5	7.9	6	3.5	0

Table 3.3 Obstacle gain as a function of the depth of the field-strength oscillations above the obstacle

E_2/E_1	1				
α/β	0.2	0.4	0.6	0.8	1.0
Obstacle gain G_o dB	10.8	7.04	5.26	4.2	3.5

Table 3.4 Obstacle gain as a function of damping factor α

In the same way as the two tables above give the obstacle gain for various depths of the field strength oscillations and for various damping factors, figures 3.24 and 3.25 show the whole spectrum in the diffraction angle range from 0 to some 20 milliradians.

We see from figure 3.24 that the higher the damping factor (for a given period $L = \lambda/\beta$ of the field strength oscillations), the lower is the obstacle gain.

Figure 3.25 shows the effect of varying the oscillation period, L. We see that changing L results in a change in the direction of maximum diffraction whereas the obstacle gain remains constant since E_2/E_1 and α/β are kept constant.

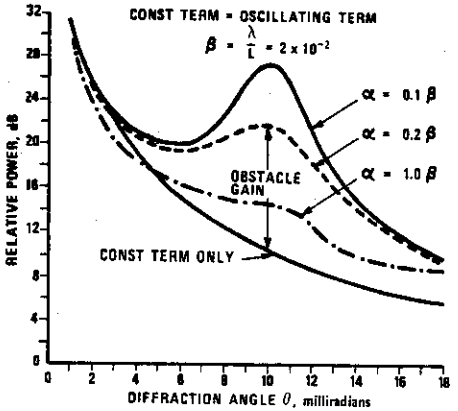

Figure 3.24 Angular diffraction spectrum for various damping factors α

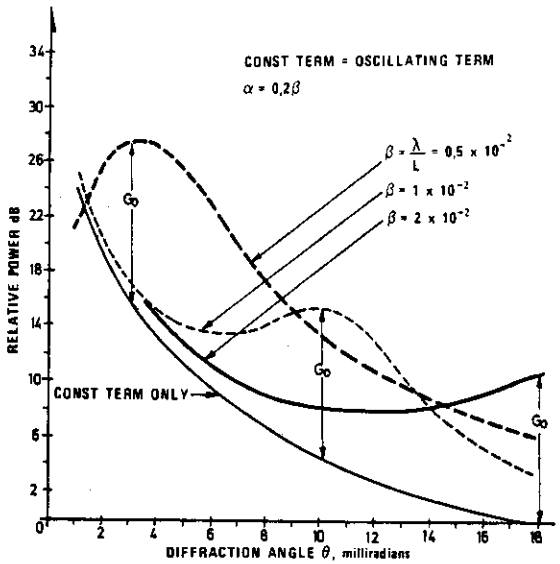

Figure 3.25 Angular diffraction spectrum for various periods of field-strength oscillations

We have shown that a terrain obstacle within line of sight gives rise to a well-defined beaming of the diffracted power behind the obstacle. The direction in which the power is beamed is determined by factors such as the height above ground of the transmitting antenna. The path loss can be greatly reduced by applying general adaption schemes.

The theoretical approach on which the numerical results are based is very simple. Knowing the path and obstacle geometry and knowing the properties of the reflecting ground, the diffracted power spectrum can readily be optimized.

Bandwidth limitations of a transmission path involving diffraction

Having formed the bases for calculating the path loss and obstacle gain, we shall now consider the bandwidth-limitations of a transmission path involving diffraction. Like in the sections above, the aim is to provide a method which first of all is physically interpretable and which makes it possible to form an opinion as to the relative importance of the various factors involved. Secondly, the aim is to form the basis for approximate calculations.

In section 2.1 above, we saw that the bandwidth of a transmission circuit is directly determined by the delay function. Knowing the delay function, the bandwidth function (power spectrum) is obtained directly from the delay function by a simple Fourier transformation process. Referring now to figure 3.26 we see that if the illuminated area above the obstacle is wide, the delay function will be correspondingly wide, and the bandwidth function will be narrow. We shall now consider the case where the illumination is limited to an antenna pattern of width β with elevation angle $\theta/2$ such that the total diffraction angle for a symmetrical path will be θ.

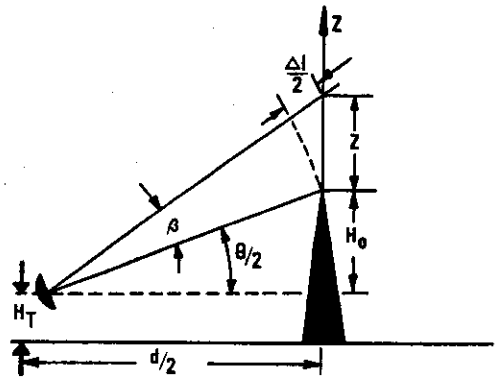

Figure 3.26 Simple path geometry for a transmission path involving knife-edge diffraction

From simple geometry we see that the path length difference is given by

$$\Delta\ell = d/2\ (\theta\beta + \beta^2)$$

$$\theta = \frac{4H_o}{d}$$

and

$$\beta = \frac{2z}{d}$$

$$\therefore \quad \Delta\ell = \frac{2}{d}\ (2H_o z + z^2) \qquad (3.59)$$

Having obtained the simple relationship between path length and ray geometry, let us return to figure 3.23. Let us again assume that the field strength distribution above the obstacle is characterized by a damped sinusoidal oscillation superimposed on an unit step function.

Let us denote the spatial period of the oscillations as δz and the damping function Δz. As we have seen in the section above, two limiting cases are of particular interest: First we assume that the ground reflections are such that the oscillating term (E_2 in Figure 3.23) dominate over the constant term E_1. In this case we essentially have a diffracting grating with line spacing δz. The object now is to calculate the bandwidth of such a diffraction circuit. As we have noted from the sections above, the center frequency in the bandpass filter is

$$F_o = \frac{c}{\delta\ell}$$

where $\delta\ell$ is the increase in path delay associated with a vertical displacement δz. From eqn (3.59) above, we have already established the relationship between $\delta\ell$ and δz. Making use of this, we find that the center frequency of our filter is given by:

$$F_o = \frac{c}{\frac{2}{d}(2H_o\delta z + \delta z^2)} \qquad (3.60)$$

As we have seen in the sections above, we can calculate δz directly from the path geometry. If H_T be the height of the transmitting antenna above the reflecting plane, then

$$\delta z = \frac{\lambda d}{4 H_T} \qquad (3.61)$$

Making use of this relationship, the expression for the center frequency of our bandpass filter becomes

$$F_o = \frac{C H_T}{H_o \lambda + \frac{\lambda^2 d}{8H_T}} \qquad (3.62)$$

Then let us calculate the width of this bandpass filter. As we have already seen (eqn (2.10) in section 2.1 above, and figure 2.3), we have learned that if the delay function is an exponentially damped sinusoid with 1/e width equal to $\Delta\ell$, and the half power width of the resulting bandpass filter is equal to

$$\Delta F_{\frac{1}{2}} = 0.16 \frac{c}{\Delta\ell} \qquad (3.63)$$

Accordingly, we find the bandwidth $\Delta F_{\frac{1}{2}}$ in the same way as we found the center frequency F_o above by substituting for $\Delta\ell$ using the appropriate value for Δz.

If the geometry is such that

$$2H_o\,\delta z >> \delta z^2$$

which requires

$$H_o H_T >> \frac{\lambda d}{8}$$

then the expression for the center frequency F_o (eqn (3.62) above) deduces to

$$F_o = \frac{c}{\lambda}\frac{H_T}{H_o} \qquad (3.64)$$

If we then express the width of the exponential damping function Δz in terms of the relation period δz as

$$\Delta z = n \cdot \delta z ,$$

our bandwidth becomes:

$$\Delta F_{\frac{1}{2}} = \frac{0.16}{n}\frac{c}{\lambda}\frac{H_T}{H_o} \qquad (3.65)$$

Note the factor n is determined by factors such as the rate at which the reflection coefficient of the ground decreases with increasing angle of incidence. This is shown in figure 3.27.

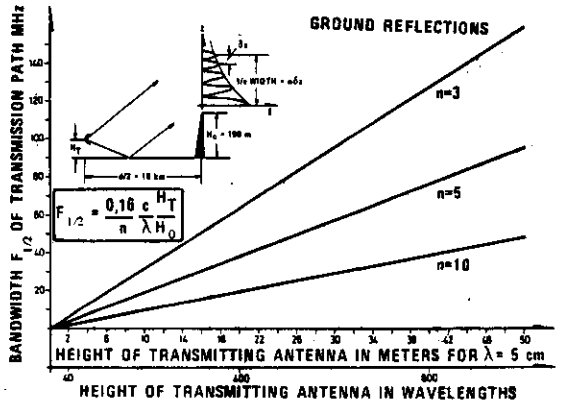

Figure 3.27 Bandwidth versus height of transmitting antenna for a diffraction path involving ground reflections. The example is for a path length of 20 km and obstacle height is 100 m

Then consider the case with no ground reflections. We illuminate the area above the obstacle by means of an antenna beam the width of which is β. The width of the delay function is then directly given as:

$$\Delta\ell = \frac{d}{2}(\theta\beta + \beta^2)$$

$$= \frac{2}{d}(2H_o z + z^2) \qquad (3.66)$$

If we assume a gaussian distribution of radiated power through the antenna beam, the half power half bandwidth is given by

$$\Delta F_{\frac{1}{2}} = 0.37\,\frac{c}{\Delta\ell} \qquad (3.67)$$

Expressing now the vertical extent z of the illuminated area above the obstacle as $z = d/2 \cdot \beta$ the half power beamwidth is

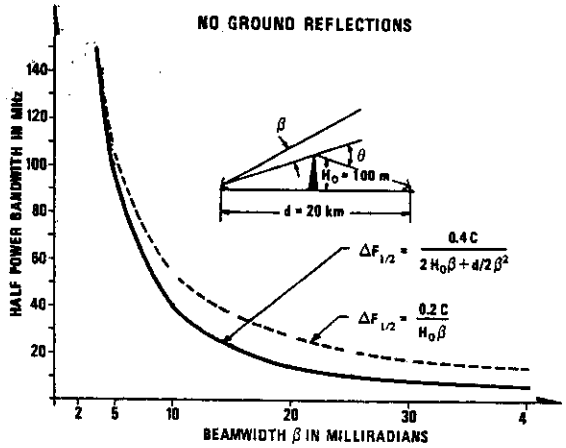

Figure 3.28 Bandwith versus beamwidth for a diffraction path with no ground reflections. The example is for a pathlength of 20 km and obstacle height is 100 m

given by

$$\Delta F_{\frac{1}{2}} = \frac{0.37\,c}{2H_o\beta + \frac{d}{2}\beta^2} \qquad (3.68)$$

This is shown in figure 3.28.

This equation suggests that the bandwidth of the diffraction path diminishes as the beamwidth increases.

When we increase the beamwidth β, the situation arises where the "effective beamwidth" is determined by the diffraction process and not by beam geometry. With no ground reflections we have shown that the scattered field falls off inversely with diffraction angle θ.

Writing then the angular power spectrum of the diffracted wave as $P \sim \theta^{-2}$, we have:

$$\frac{P(\theta)}{P(\theta_o)} = \left(\frac{\theta_o + \Delta\theta}{\theta_o}\right)^{-2}$$

Then let us define the "effective beamwidth" as the angular region within which the diffracted power is larger than 1/10 of the maximum power obtained for the minimum diffraction angle $\theta_o = \frac{2H_o}{d/2}$. We then have:

$$\frac{P(\theta)}{P(\theta_o)} = \frac{1}{10} = \left(\frac{\theta_o + 2\beta_{eff}}{\theta_o}\right)^{-2}$$

$$\therefore \quad \beta_{eff} = \frac{\theta_o}{2}(\sqrt{10} - 1)$$

$$= \frac{2H_o}{d}(\sqrt{10} - 1)$$

Referring to the example illustrated in figure 3.28, this means that as the beamwidth increases, the bandwidth will approach a limit given by the following expression:

$$(\Delta F_{\frac{1}{2}})_{LIM} = \frac{0.37\ c}{2H_o\ \beta_{eff} + \frac{d}{2}\ \beta_{eff}^2}$$

Inserting the appropriate numbers for obstacle height H_o and range d, we find that the limiting bandwidth is 12 MHz.

If we are dealing with large antennas, such that β is small, and if the height of the obstacle, H_o is large, the expression for bandwidth reduces to

$$\Delta F_{\frac{1}{2}} = \frac{0.18\ c}{H_o\ \beta} \qquad (3.69)$$

Finally, figure 3.29 summarizes the section on bandwidth properties of a transmission path involving knife edge diffraction.

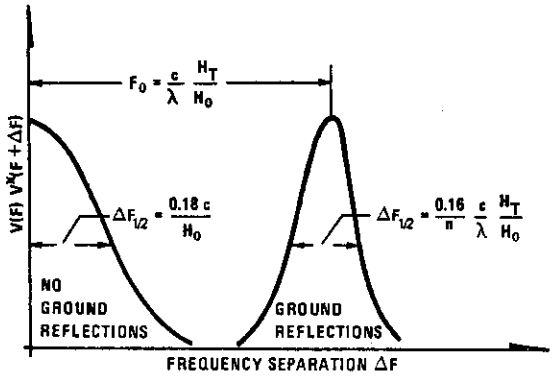

Figure 3.29 Bandwidth properties of a transmission path involving knife-edge diffraction

From the summarizing figure 3.29 we see that if no ground reflections are involved, the transmission circuit will act as a lowpass filter (maximum at carrier frequency). If, however, ground reflections are involved, the field-strength distribution above the obstacle will be periodic giving rise to a bandpass filter which is not centered at the carrier frequency. This phenomenon is treated in some detail in chapter 2.1, the results of which are summarized in figure 2.3. Here we see that a periodic delay function results in a frequency covariance function which is displaced from the carrier frequency.

From the two preceding sections, we have shown that it is possible to minimize the transmission loss by adjusting the height of the transmitting antenna (measured in wavelengths) so as to "beam" the diffracted wave in the desired direction. We have also shown that we can adjust the geometry so as to optimize the bandwidth of the transmission circuit. It remains to study the spatial correlation properties of the scattered field. In chapter 2.2 we have shown that if we are to analyse an object, we shall have to produce an illuminating field which is coherent both as regards phase and amplitude across the object. This means that if the height of the target to be analysed is ΔH, we shall have to organize ourselves so as to produce an illuminating field which is coherent over the vertical region ΔH.

We shall now calculate the vertical correlation properties of fieldstrength at the receiving site of a transmission path involving knife-edge diffraction. We shall base these calculations on the conclusions of earlier sections (in particular section 2.2 and section 3.2.4). Based on these earlier findings, we can derive accurate expressions if we base our calculations on regular Fourier transforms.

We shall now apply an approximate method based on semi-intuitive arguments so as to ensure a detailed physical understanding of the principles involved.

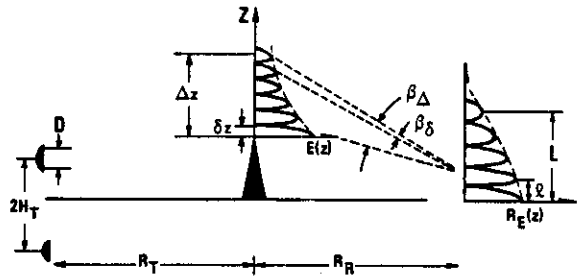

Figure 3.30 Spatial correlation of field-strength at the receiving sight of a transmission path involving knife-edge diffraction

From figure 3.30 we see that a transmitting antenna produces a periodic field strength distribution above the obstacle when ground reflections are involved. If the ground acts as a perfect mirror, the transmitter can be visualized as having two antennas with vertical spacing H_T giving rise to a set of antenna lobes of beamwidth $\frac{\lambda}{2H_T}$. If we are dealing with antennas of diameter D, these antenna lobes will not be of the same intensity, but have the appearance of damped oscillations. The width of this damping function is determined by the antenna aperture such that the width of the envelope will be $\frac{\lambda}{D}$.

Hence:

$$\delta z = \frac{\lambda}{2H_T} R_T$$

and

$$\Delta z = \frac{\lambda}{D} R_T$$

Having obtained qualitative information about the fieldstrength distribution above the obstacle, let us now discuss what this will lead to at the receiving site. The shortest scale to be observed in the vertical fieldstrength distribution at the receiver, is associated with the widest angular distribution (as we have seen from section 2.2 above). Conversely, the largest scale is associated with a narrow angular distribution.

Viewing the diffracting screen from the receiving end, we will observe an angle of arrival-spectrum with many lobes. As depicted in figure 3.30, the overall width of the angular spectrum is therefore:

$$\beta_\Delta = \frac{\Delta z}{R_R} = \frac{\lambda R_T}{D R_R} \qquad (3.70)$$

and simularly

$$\beta_\delta = \frac{\delta z}{R_R} = \frac{\lambda R_T}{2H_T R_R} \qquad (3.71)$$

We have already seen that an antenna with aperture D produces a beam the width of which is

$$\beta = \frac{\lambda}{D}$$

by pure reciprocity considerations, therefore, an angle of arrival-spectrum of width β will produce a fieldstrength distribution the width of which is

$$L = \frac{\lambda}{\beta}$$

We know, of course, that this is only approximately correct. If we want an accurate expression, the angular power spectrum is obtained as the Fourier transform of the fieldstrength distribution over the aperture. In the same way as the spatial correlation of fieldstrength is obtained by Fourier transforming the angular power spectrum. Making use of these simple qualitative results, we find that the fine-scale spatial correlation distance of the diffraction field is

$$\ell = \frac{\lambda}{\beta_\Delta} = D \frac{R_R}{R_T} \qquad (3.72)$$

similarly the large scale correlation distance is:

$$L = \frac{\lambda}{\beta_\delta} = 2H_T \frac{R_R}{R_T} \qquad (3.73)$$

Intuitively this is rather obvious: For a symmetrical path ($R_R = R_T$) the fine-scale fieldstrength structure is the same as the aperture of the transmitting antenna whereas the large scale structure is equal to twice the antenna height, which of course is the equivalent antenna aperture of a transmitting system involving ground reflections.

If we have no ground reflections, the correlation distance of fieldstrength at the receiving sight will be

$$\ell = D \frac{R_R}{R_T} \qquad (3.74)$$

In conclusion, we should note that the spatial correlation properties of the diffracted field is determined entirely by the path geometry, and by the size and the positioning of the transmitting antenna.

4 BIBLIOGRAPHY

1. Gjessing, Dag T. "Remote Surveillance by Elektromagnetic Waves for Air-Water-Land", Ann Arbor Science Publishers Inc., Michigan, USA (1978)
2. Gabriel, William F. "Adaptive Arrays - An Introduction", IEEE Proceedings, Vol 64, No. 2 (Feb 1976)
3. Applebaum, S. "Adaptive Arrays", IEEE Transactions on Antennas and Propagation, Vol AP-24, No. 5, pp. 585-589 (Sep 1976)
4. Stratton, J.A. "Electromangetic Theory", New York: McGraw-Hill (1941)
5. Megaw, E.C.S. "Fundamental Radio Scatter Propagation Theory", Proceedings IEE Monograph no. 236 R (May 1957)
6. Batchelor, G.K. "The Scattering of Radio Waves in the Atmosphere by Turbulent Fluctuations in Refractive Index", Research Report no. EE262 (1955), School of Engineering, Cornell University
7. Bass, F.B., I.M. Fuks "Wave Scattering from Statistically Rough Surfaces", Pergamon Press (1979)
8. Wiener, N. "Generalized Harmonic Analysis", Acta Math 55 (1930)
9. Gjessing, Dag T. "Environmental Remote Sensing; Part I: Methods Based on Scattering and Diffraction of Radio Waves", Physics in Technology Vol 10 (1979)
10. Gjessing, Dag T. "Atmospheric structure deduced from the forward scatter wave propagation experiments", Radio Sc.
11. Bean, B.R., E.J. Dutton. Radio Meteorology, US Dept of Commerce, NBS, Monograph 92, US Government Printing Office, Washington DC (1966)
12. Lee, R.W., J.C. Harp. "Weak scattering in random media", IEEE 57, p. 375 (1969)
13. Gjessing, D.T., A.G. Kjelaas, J. Nordö. "Spectral measurements and atmospheric stability", J. Atmosph. Sci. 26, 3, 462.8 (1969)
14. Gjessing, D.T., K.S. McCormick. "On the Prediction of the Characteristic Parameters of Long-Distance Tropospheric Communication Links", IEEE Trans Comm 22, 9 (Sept 1974)
15. Gjessing, D.T. "On the Use of Forward Scatter Techniques in the Study of Turbulent Stratified Layers in the Troposphere", Boundary-Layer Meteorol 4, pp. 377-396 (1973)
16. Gjessing, D.T. "An Experimental Determination of the Spectrum of Permittivity and Air Velocity Fluctuations along a Vertical Direction in the Troposphere using Radio Propagation Methods", J. Atmosph. Terr. Phys. 26, 2 (Febr 1964)
17. Bull, G., J. Neisser. "Untersuchungen der atmosfärischen Feinstruktur mit Hilfe von Ausbreitungsmessungen im Mikrowellenbereich", Beitr Geophys 77(5), pp. 394-410 (1968)
18. Eklund, F., S. Wicherts. "Wavelength Dependence of Microwave Propagation Far Beyond the Radio Horizon", Radio Sci 3(11), pp. 1068-1074 (1968)

19. Fehlaber, L. Fernmeldetechnisches Zentralamt, Deutschen Bundespost, "Diversity Abstand auf Scatter Strecken im Frequenzbereich Zwischen 1 GHz und 10 GHz", Tech Vericht 5581 (1966)
20. Fehlaber, L., J. Grosskopf. Fernmeldetechnisches Zentralamt, Deutsche Bundespost, "Messung der Gewinnmindering bei 1715 MHz auf einer 409 km langen Scatter-Versuchusstrecke", FTZ, A455, Tb 7 (1968)
21. Bolgiano, R. Jr., Cornell University. "A study of Wavelength Dependence of Transhorizon Radio Propagation", Res. Rep. 188 (1964)
22. Cox, D.C., A.T. Watermann, Jr, "Phase and Amplitude Measurements of Transhorizon Microwaves with a Multidata-Gathering Antenna Array", AGARD Conf. Proc. 37, 18-1 to 18-6 (1968)
23. Gjessing, D.T. "Scattering of Radio Waves from Regular and Irregular Time Varying Refractive-Index Structures in the Troposphere", AGARD Conf Proc 37, 15-1 to 17-17 (1968)
24. Grosskopf, J. "Investigation of the Receiving Field for Scatter Propagation", AGARD Conf. Proc. 37, 22-1 to 22-11 (1968)
25. Gjessing, D.T., J.A. Börresen. "The Influence of an Irregular Refractive-Index Structure on the Spatial Field-Strength Correlation of a Scattered Radio Wave", IEE (Lond.) Conf. Pub. 48, pp. 43-50 (1968)
26. Gjessing, D.T. "Scattering mechanisms and channel characterization in relation to broad-band radio communication systems", AGARD Conference Proceedings CP-244, Cambridge USA (Oct 1977)
27. Hall, M.P.M. Appelton Laboratory, UK, Private communication
28. Wait, J.R. "A Note on VHF Reflection from a Tropospheric Layer", Radio Sc. 7, 847-848 (1964)
29. Lumley, J.L. "Theoretical aspects of research on turbulence in stratified flows". Atmospheric turbulence and radio wave propagation, editor A.M. Yaglom and V.I. Tatarsky. Publishing House NAUKA, Moscow, pp. 105-112 (1967)
30. Waterman, A.T. Jr., D.T. Gjessing, C.L. Liston. "Statistical Analysis of Transmission Data From a Simultaneous Frequency- and Angle Scan Experiment", Paper presented at the URSI Spring Meeting, Washington D.C. (1961)
31. McGillem, C.D., C.R. Cooper, W.B. Waltman. "Use of Wideband Stochastic Signals for Measuring Range and Velocity", Easton 69 Record, 305-311 (1969)
32. Ottersten, H., K.R. Hardy, C.G. Little. "Radar and Solar Probing of Waves and Turbulence in Statically Stable Clear-Air Layers", Boundary-Layer Meteorol, this issue, p. 47-89 (1973)
33. Saxton, J.A., J.A. Lane, R.W. Measows, P.A. Matthews. "Layer Structure of the Troposphere", Proc. IEEE 111, 2 (1964)
34. Gjessing, D.T. "Radiophysical aspects of irregular structure in the atmosphere". Atmospheric turbulence and radio wave propagation, editor A.M. Yaglom and V.I. Tatarsky. Publishing House NAUKA, Moscow, pp. 105-112 (1967)

35. Seehars, H.D. "Investigation of the Dielectric Turbulence and Wind Stratification in the Troposphere by Means of SHF Beamswinging Experiments over Sea", Berichte Nr. 18 des Instituts für Radiometeorologie und Maritime Meteorologie an der Universität Hamburg (1970)
36. Gjessing, D.T., H. Jeske, N. Klint-Hansen. "An Investigation of the Tropospheric Fine Scale Properties Using Radio, Radar and Direct Methods", J. Atmosph. Terr. Phys. 31, pp. 1157-1182 (1969)
37. Gjessing, D.T., F. Irgens. "Scattering of Radio Waves by a Moving Rippled Layer: A Simple Model Experiment", IEEE Trans Antennas & Propagation AG-12, 6 (1964)
38. Kerr, D.E. "Propagation of Short Radio Waves", Dover Publication (1965)
39. McCormick, G.C., A. Ivendry. "Depolarization over a Link due to Rain, Measurement of Parameters", Radio Science 11, pp. 741-749 (1976)
40. Drufuca, G. "Rain Attenuation Statistics for Frequencies above 10 GHz from Raingauges Observations", J. de Rech. Atm. 8, 1-2, pp. 399-411 (1974)
41. Ratcliffe, J.A. "Some Aspects of Diffraction Theory and their Application to the Ionosphere", The Physical Society Reports on Progress in Physics 19, 188 (1965)
42. Gjessing, D.T. "Adaptive Radar in Remote Sensing", Ann Arbor Science Publishers Inc., Michigan, USA (1981)